

LA-3612

c. 2

**LOS ALAMOS SCIENTIFIC LABORATORY**  
of the  
**University of California**  
LOS ALAMOS • NEW MEXICO

**Criticality Data and Factors Affecting Criticality  
of Single Homogeneous Units**

LOS ALAMOS NATIONAL LABORATORY



3 9338 00314 6098

**DO NOT CIRCULATE**

**PERMANENT RETENTION**

**REQUIRED BY CONTRACT**

UNITED STATES  
ATOMIC ENERGY COMMISSION  
CONTRACT W-7405-ENG. 36

## LEGAL NOTICE

This report was prepared as an account of Government sponsored work. Neither the United States, nor the Commission, nor any person acting on behalf of the Commission:

A. Makes any warranty or representation, expressed or implied, with respect to the accuracy, completeness, or usefulness of the information contained in this report, or that the use of any information, apparatus, method, or process disclosed in this report may not infringe privately owned rights; or

B. Assumes any liabilities with respect to the use of, or for damages resulting from the use of any information, apparatus, method, or process disclosed in this report.

As used in the above, "person acting on behalf of the Commission" includes any employee or contractor of the Commission, or employee of such contractor, to the extent that such employee or contractor of the Commission, or employee of such contractor prepares, disseminates, or provides access to, any information pursuant to his employment or contract with the Commission, or his employment with such contractor.

This report expresses the opinions of the author or authors and does not necessarily reflect the opinions or views of the Los Alamos Scientific Laboratory.

**LOS ALAMOS SCIENTIFIC LABORATORY**  
**of the**  
**University of California**  
LOS ALAMOS • NEW MEXICO

Report written: July 1964

Report distributed: September 22, 1967

**Criticality Data and Factors Affecting Criticality**  
**of Single Homogeneous Units**

by

W. R. Stratton



## CONTENTS

	Page
Abstract	3
I Introduction	3
II Shape Conversion	7
III Influence of Density	9
IV Internal Scattering (Dilution by Nonmoderators)	12
V Internal Moderation	
(Hydrogen, Carbon, and Oxygen)	14
A. U(93.5): Metal-Water-Graphite and Oxide-Water Cores	15
B. Uranium Enriched to Thirty Percent, U(30)	22
C. Uranium Enriched to Five Percent, U(5)	25
D. Uranium Enriched to Three Percent, U(3)	27
E. Uranium Enriched to Two Percent, U(2)	28
F. Uranium Enriched to 1.42 Percent, U(1.42)	30
G. Uranium Enriched to 1.03 Percent, U(1.03)	31
H. <sup>233</sup> U Systems	31
I. Plutonium Systems	34
VI Internal Moderation	
(Deuterium, Beryllium, and Oxygen)	37
VII Reflectors	38
A. Thickness, Gaps, Density	38
B. Thick Moderating Reflectors	
(Metastable Systems)	47
VIII Neutron Poisons	48
IX Summary and Conclusions	50
Acknowledgments	50
References	51

CRITICALITY DATA AND FACTORS AFFECTING CRITICALITY  
OF SINGLE HOMOGENEOUS UNITS

by

W. R. Stratton

ABSTRACT

The critical parameters of single homogeneous units are examined and tabulated. The study includes both theoretical and experimental results which are compared extensively in order to establish the accuracy of the theoretical method. The experimental data are reduced to standard conditions to facilitate this comparison and to investigate the consistency of the large number of critical experiments.

Given the validity of the calculational scheme, the various affects of diluents (including moderators), reflectors, density charges, and poisons are studied. Finally, by application of the theory, results are obtained which are inaccessible or very difficult to obtain by experimental methods.

---

I. INTRODUCTION

The critical dimensions of mixtures of enriched uranium or plutonium metals with water were first estimated in 1942,<sup>(1)</sup> and by early 1943 calculations<sup>(2)</sup> and improved cross sections suggested that the spherical and unreflected critical mass of pure  $^{235}\text{U}$  metal was 60 kg, while reflectors of normal uranium and gold reduced the requirements to 15 and 22 kg, respectively. The uranium reflected number was amazingly good (experimental value<sup>(3)</sup> = 16.65 kg), while the predicted bare critical radius was larger than the best modern value<sup>(3)</sup> by only 7%; the estimate for the gold reflector stands unchallenged. The first experimental homo-

geneous critical assembly was the Los Alamos "LOPO"<sup>(4,5)</sup> -- the Low Power Boiler -- which was a BeO-reflected, 14.95-liter, stainless steel sphere filled with a solution of uranyl sulfate. The enrichment was 14.67%, and the critical state was first achieved with a  $^{235}\text{U}$  mass of 565 g on May 9, 1944.

Since these early and historic occasions, critical data for single homogeneous units, both theoretical and experimental, from many sources, and of wildly varying degrees of precision, usefulness, and accessibility have been accumulating at a prodigious rate. In this paper I propose to consider a much smaller set, only those critical data that can be considered "basic." By basic is implied some simplicity

in geometry and, hopefully, minimal components and complexity in the experiments. In addition, prejudice is shown in favor of experiments which can be generalized, i.e., which can be correlated by varying one or two parameters to form a part of an internally consistent set. Unless we are desperate for experimental data, those experiments that are not simple in reflection, core composition, etc., will not be considered. Experiments may be most carefully performed, but be so highly specialized as to be quite useless for our purposes. Generally a core will be required to be a simply connected volume with plane or convex surfaces, even though the more complicated shapes are often of much practical importance.

The presentation will, in large part, be organized around the results of a theoretical parametric survey of critical data, and, indeed, many of the critical dimensions given in the tables will be from this source. The calculation is the Carlson Sn code<sup>(6-9)</sup> as prepared for the IBM 7094 computer, while the neutron cross-section set is that of 16 energy groups created by Hansen and Roach.<sup>(10)</sup> Other theoretical surveys of critical data have been published (see as examples, References 11 through 14), but these will not be discussed; comparison will be made only to experiments. In this article, mention of theory, unless otherwise modified, invariably implies the Carlson method and Hansen-Roach cross sections.

The cross-section set was designed for fast and intermediate critical assemblies, but, as will be developed, is equally applicable to thermal systems. Generally the  $S_4$  approximation was utilized, except for thin slab calculation in which the better representation of  $S_8$  was sometimes needed. The  $S_4 - S_8 - S_{16} \dots$  convergence pattern was investigated to a limited extent. The pattern for the extant code seems similar to that found in 1958<sup>(9)</sup> for spheres and slabs, but qualitatively dissimilar for

cylinders. I note, however, that these convergence patterns are most significant for small (or thin) cores and that the number of space points in a core may be of equal or greater importance in determining accuracy. I also observe<sup>(15)</sup> that, since  $S_4$  and  $S_8$  are the most commonly used approximations, choice of cross sections may have been prejudiced, though not consciously or conspicuously, in favor of  $S_4$  or  $S_8$ . The number of significant figures retained in the several tables for the critical parameters represents not precise knowledge so much as use of a computer. Calculated results should be internally consistent to the precision quoted.

Such computed data, as obtained by application of an elaborate theory, are relevant to the real world of reactors, critical assemblies, chemical processing plants, storage and transportation problems, etc., only if a comparison of calculational results to experimental data is convincingly done. This is attempted throughout, but primarily in the latter sections, and, whenever possible, the deviation of theoretical data from experiment will be noted. This comparison not only serves to measure the accuracy of such calculations with the cross sections needed for input to the theory, but also casts some light upon the internal consistency of the vast body of experimental data. Given the validity of the scheme, additional benefits which may now be believable arise from the possibility of calculating critical (or supercritical) points that are either impossible or most difficult to reproduce experimentally and of conducting parametric studies at a substantially reduced cost. Given an internally consistent set of data, one can hope to uncover simple regularities which can lead to additional generalizations, seriously needed in this field. I note that final recourse must always be to experiment.

In the most general terms, the critical size of a given system is sensitive to the allowable neutron leakage, moderation,

and poison. Neutron leakage is often subdivided into the effects of shape, density, internal scattering (including dilution effects), and external scattering (reflection). These several items are most difficult to disentangle completely, and a fully logical presentation in which no prior knowledge of critical data is assumed seems to be nearly impossible. As minimum prerequisites, an awareness of the capabilities of experimental methods and a feeling for the power of modern computational techniques will be expected along with some limited knowledge of critical data, of those factors affecting criticality, and of some few concepts from elementary theory.

Ideally, one hopes first to understand the simplest systems and later to extend one's knowledge through application of simple transformations to more complicated geometries and multiphase mixtures. This is not completely possible, but will be attempted, at least in part. As a beginning, and to serve as a conceptual handle or as a vehicle with which to follow the development, the simplest and most basic critical data -- those pertinent to isolated fissile metal spheres -- will be presented, and these systems will then be imagined to be surrounded by thick reflectors of water and natural uranium. These several anchor points will then be distorted by changes of shape and density, and modified by dilution with nonmoderators and moderators. The several subdivisions will be treated rather quickly in order to lead rapidly to the major block of critical data, those for fissile metal-water and fissile metal-water-

graphite cores; and a fairly painstaking comparison of theoretical and experimental results will be presented with this information. Following this section, some special characteristics and effects of reflectors will be given, and miscellaneous details passed over earlier will be discussed. Finally, some information on poisons will be offered, but this coverage will be somewhat arbitrary and cursory.

The basic critical data referred to above should be those for isolated, metal spheres of the fissile\* isotopes --  $^{235}\text{U}$ ,  $^{233}\text{U}$ , and  $^{239}\text{Pu}$ . However, as the pure isotopes are not generally available, we meet our first rebuff and note that critical experiments are customarily performed with fissile metals diluted with fissionable\* (primarily  $^{234}\text{U}$ ,  $^{238}\text{U}$ , and  $^{240}\text{Pu}$ ) isotopes. Plutonium is a special case, often fabricated with about one atomic percent gallium which is added to stabilize the metal in the high temperature delta phase. Thus the critical data for our starting point apply to isolated (unreflected) metal spheres of slightly impure fissile isotopes. These data<sup>(3)</sup> along with pertinent densities, impurities, and theoretical radii are listed in Table I.

The theory is the Carlson Sn Method (in these cases the  $S_0$  approximation) using the Hansen-Roach 16-group, cross-section

\*The meanings attached to the words fissile and fissionable will be those suggested by Everitt Blizard in his editorial in the March 1961 issue of Nuclear Science and Engineering. Fissile implies  $^{233}\text{U}$ ,  $^{235}\text{U}$ ,  $^{239}\text{Pu}$ ,  $^{241}\text{Pu}$ , etc., while fissionable includes  $^{234}\text{U}$ ,  $^{236}\text{U}$ ,  $^{238}\text{U}$ ,  $^{240}\text{Pu}$ , etc.

TABLE I. CRITICAL DATA FOR ISOLATED METAL SPHERES

Core Material	Density (g/cm <sup>3</sup> )	Experimental Radius (R <sub>Exp</sub> ) (cm)	Mass (kg)	Theoretical Radius (R <sub>DSN</sub> )	$\frac{R_{DSN}}{R_{Exp}}$	Principle Diluents
U(93.8)	17.60	8.710	48.714	8.739	1.0033	$^{238}\text{U}$
Pu(95.5)	14.92	6.285	15.516	6.298	1.0021	$^{240}\text{Pu}$
$^{233}\text{U}$ (98.1)	18.10	5.965	16.091	5.949	0.9973	$^{234}\text{U}$ , $^{238}\text{U}$

set. The calculation produces results tolerably close to the experimental values as is indicated by the ratio of theoretical to experimental radii. Historically, the Hansen-Roach set was constructed to contain only six groups; <sup>(10)</sup> best microscopic cross sections were employed, and the metal systems in Table I (and those in the upper half of Table II) were used as check points. To the extent that group constants were adjusted (but only within quoted experimental error) to allow a reasonable calculation of critical data, the agreement noticed in Table I is not accidental.

Some conventions started in Table I are worth noting for the sake of clarity. The notation U(93.5), U(4.9), etc., means uranium enriched to 93.5% <sup>235</sup>U by weight, 4.9% <sup>235</sup>U by weight, etc. Where appropriate, the same scheme will be used for plutonium and <sup>233</sup>U; for example, Pu(96) will imply plutonium in which 96% by weight is <sup>239</sup>Pu and <sup>241</sup>Pu and 4% is <sup>240</sup>Pu and <sup>242</sup>Pu, with the rest assumed to be negligible unless otherwise stated. To avoid confusion between <sup>235</sup>U and <sup>233</sup>U, the superscript <sup>233</sup> will invariably be attached, while for <sup>235</sup>U the superscript will be omitted, except when needed for clarity. In the several tables, the quoted densities and critical masses refer specifically to the fissile

isotope. Generally, comparison of theory and experiment will be given as a ratio of dimensions as in Table I.

A basic concept in reactor physics is that of a reflector or (historically) a tamper -- something that returns a certain fraction of the escaping neutrons to the core. This conservation of neutrons permits a reduction in the amount of fissile material required to maintain the critical state, the reduction depending upon the thickness and the material of the reflector. The change in mass requirement is often described as a "reflector saving" -- the physical decrease of core dimension allowed by introduction of the reflector. This change,  $\Delta R$ , can be expressed conveniently as a length or, less commonly, as a mass/unit area. Ramifications of this subject are nearly endless (details on reflectors will appear in Section VII), but, for our purposes, critical data for thick, natural uranium-reflected and thick, water-reflected metal spheres of the fissile isotopes are presented in Table II.<sup>(3)</sup> These particular reflectors are "thick" in the sense that the system is saturated; additional material will not further reduce the critical radius, hence, the reflector is effectively unbounded or "infinite".

For the uranium-reflected cores, the

TABLE II. CRITICAL DATA FOR REFLECTED METAL SPHERES

Core Material	Density (g/cm <sup>3</sup> )	Experimental Radius (R <sub>Exp</sub> ) (cm)	Mass (kg)	Theoretical Radius (R <sub>DSN</sub> )	$\frac{R_{DSN}}{R_{Exp}}$	Reflector Saving (cm)
Uranium Reflection						
U(93.2)	17.443	6.119	16.746	6.120	1.00016	2.67
Pu(95.2)	14.619	4.513	5.629	4.524	1.0024	1.77
<sup>233</sup> U(98.8)	18.121	4.217	5.692	4.213	0.99905	1.75
Water Reflection						
U(93.9)	17.372	6.690	21.788	6.756	1.00997	2.10
Pu(100)	19.70	—	—	3.983	—	0.92
<sup>233</sup> U(100)	18.70	—	—	4.500	—	1.24



agreement between theory ( $S_8$ ) and experiment is excellent, but, as discussed above, not entirely accidental. The experimental data for water reflection are less extensive, and, as noted in Table II, the calculation ( $S_8$ ) is not quite so accurate but still quite satisfactory. Water-reflected experiments are difficult, and such information for Pu and  $^{233}\text{U}$  is lacking (the calculation for these two employed the  $S_4$  approximation). These water-reflected data are the first for which the full 16-neutron energy groups are needed. The neutron's energy upon returning to the core can have been drastically reduced -- by a factor of  $10^8$ , for example -- but even such a radical change is described without difficulty.

## II. SHAPE CONVERSION

For an unreflected system, criticality is governed by neutron leakage through the surface; and, because the sphere has the smallest surface-to-volume ratio of any geometry, this shape should give the minimum critical volume. This, indeed, is the case, and much experimental and theoretical critical data are obtained from the study of spherical systems. An often more convenient geometry for experiments (but never for theory) is a right circular cylinder or parallelepiped. The need to convert information from one shape to another is apparent, and a means for doing this utilizes buckling expressions as are derived in reactor theory, <sup>(16)</sup> wherein the buckling,  $B^2$ , is defined by

$$B^2 = \left( \frac{\pi}{R_{sp} + \delta_{sp}} \right)^2 + \left( \frac{J_0}{h + 2\delta_{sl}} \right)^2 + \left( \frac{J_0}{R_{cyl} + \delta_{cyl}} \right)^2. \quad (1)$$

In this equation  $R_{sp}$ ,  $h$ , and  $R_{cyl}$  are the sphere radius, cylinder length, and cylinder radius, respectively, and the  $\delta$ 's are the effective extrapolation distances.  $J_0 = 2.405$  is the first root of the zeroth-

order Bessel function. Often, the extrapolation distance is only weakly dependent upon geometry or fissile material diluents, and a reasonable approximation is to assume that  $\delta_{sp} = \delta_{sl} = \delta_{cyl}$ . With this approach, empirical  $\delta$ 's may be derived, and Eq. 1 becomes a most powerful tool in the treatment of experimental data. This phenomenological approach is adopted here; the scheme of Eq. 1 is accepted, and some of the critical data will be examined to find those extrapolation distances which seem most reasonable and accurate. In particular the U(93.5)-graphite-water systems (Section V) suggest that for these mixtures at normal densities, the undermoderated cores may be informed with the aid of an extrapolation distance that is only very slightly dependent upon the size, as

$$\delta = 1.83 + 0.22 \log \text{volume}, \quad (2)$$

in which equation the volume is expressed in liters and the extrapolation distance in centimeters. It is clear that precision for  $\delta$  is really important only for small cores; the best value for U(93.5) metal <sup>(17)</sup> at a total density of  $18.8 \text{ g/cm}^3$  is 2.04 cm, while for Pu( $\sim 97$ ) <sup>(15)</sup> at a total density of  $19.6 \text{ g/cm}^3$ ,  $\delta$  is 1.56 cm.

Given values of  $\delta$ , Eq. 1 immediately permits conversion of right cylinders and parallelepipeds to spheres and allows reasonable extrapolations of experimental data to infinite slabs and cylinders. The inverse is, of course, equally possible.

Most of the critical data presented will be described in the one-dimensional form because (1) these three one-dimensional geometries are amenable to accurate calculations, (2) such a scheme for reduction of data can define a method for examination of diverse experiments for internal consistency (within limitations to be developed), and (3) for many problems, these geometries provide reasonable comparisons to actual situations. These shapes are accepted as standards to which data will be converted.

For reflected systems, it is not correct to assume that the minimum critical volume is contained within a sphere. If, for example, a solid metal system is immersed in water, the fuel surface still determines the neutron leakage rate, but the surface area also determines the fission rate from thermal neutrons returning from the moderating reflector. For grossly distorted volumes, the latter fact is obviously more important, but for shapes with plane or convex surfaces, the situation is less clear. Apparently, for some under-moderated systems<sup>(18)</sup> a right circular cylinder with a height-to-diameter ratio ( $h/d$ ) of about 0.9 may have a slightly smaller critical volume than a sphere. This same effect is seen in the results of some two-dimensional neutron transport calculations.<sup>(19)</sup> These particular problems involved size calculations of thick-water-reflected cores whose composition was a fixed, under-moderated mixture of U(93.5) and water and whose geometry was that of a finite right cylinder. Given various cylinder diameters ( $d$ ), the code (Carlson Sn formulation, two-dimensional (R,Z) DDK code,<sup>(20)</sup> and Hansen-Roach 16-group cross sections) returned critical heights ( $h$ ). These data are illustrated in Fig. 1 as a ratio of cylinder core volume to sphere volume, plotted against the dimensionless ratio  $\frac{h}{d}/(1 + \frac{h}{d})$ . The minimum cylinder volume apparently is about 2.5% less than that for the sphere, with the minimum occurring at a height-to-diameter ratio of about 0.82. Results for this single, special core mixture should be generalized only with caution.

As in the case of bare cores, a scheme for converting one geometry to another can be defined if the reflector saving (see Table II) is added to the extrapolation distance, i.e.,  $\delta' = \delta + \Delta R$ . Thus,

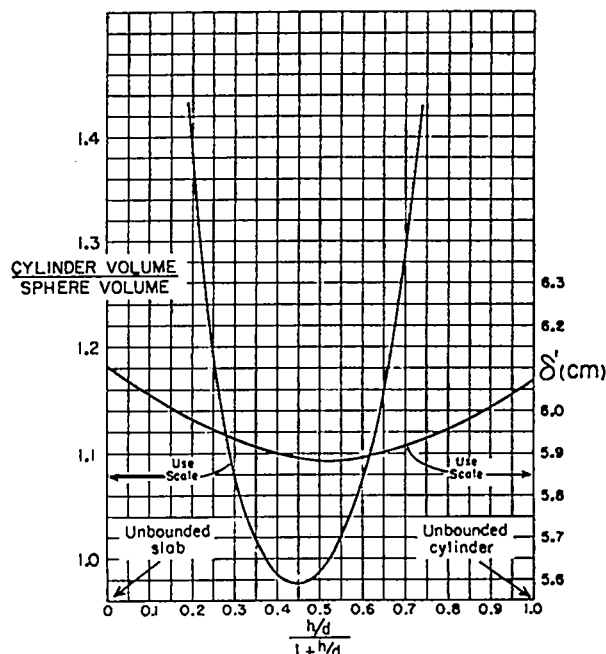


Fig. 1. (Cylinder volume)/(sphere volume) and  $\delta'$  = (extrapolation distance plus reflector saving) as functions of the dimensionless shape parameter  $\frac{h}{d}/(1+h/d)$  for water-reflected, metal-water systems whose  $H/^{235}\text{U}$  moderation ratio is about 30. These data were generated by application of the two-dimensional, as well as the one-dimensional, transport code.

$$B^2 = \left( \frac{\pi}{R_{sp} + \delta'} \right)^2 = \left( \frac{\pi}{h + 2\delta'} \right)^2 + \left( \frac{J_0}{R_{cyl} + \delta'} \right)^2 \quad (3)$$

The crucial quantity is  $\delta'$ , the sum of an extrapolation distance,  $\delta$ , and a reflector saving,  $\Delta R$ . Some information is obtained for this quantity (for water reflection) from the set of two-dimensional calculations already mentioned. These critical data, along with the one-dimensional sphere, slab, and cylinder data, are internally consistent if  $\delta' = 5.90 \text{ cm}$ <sup>(18)</sup> is used for the sphere and values of  $\delta'$  illustrated in Fig. 1 are taken to be appropriate for the other geometries; in all cases normal density is assumed.

In general, the reflector saving is dependent upon the reflector material and

thickness, the core substance, and, to some extent, the geometry of the system. Data for specific cases may be extracted from the tables that follow. For example, for the undermoderated U(93.5)-C-H<sub>2</sub>O systems (Table V), a reflector saving may be derived that is directly proportional to the radius. From these same data, a very rough inverse proportionality to the H/<sup>235</sup>U atom ratio also may be noted. For some situations, the reflector saving can be found to be large -- of the order of the core dimensions. For the very special case of the "Bell Cavity" (Section VII), the reflector saving becomes an apparently absurd, but real, 0.2 statute mile. Reasonable care in application seems appropriate.

In general these shape conversions are less precise than comparable alterations to bare cores, but for many situations they are surprisingly accurate. Data for the reflected systems, like those unreflected, will be presented in terms of the one-dimensional geometries.

### III. INFLUENCE OF DENSITY

Uniform variation of the density of a fissile system of fixed chemical composition influences the required critical mass (21) in a manner that is sometimes described as the only law in criticality physics which is simultaneously exact, simple, and useful. (22) This law states:

In a critical system, if the densities are increased everywhere to  $x$  times their initial value and all the linear dimensions are reduced to  $1/x$  times their initial value, the system will remain critical.

Thus, to maintain criticality (or maintain the same number of mean free paths), a dimension and the density must be inversely proportional, as:

$$\text{critical radius} = r_c \propto \rho^{-1}, \quad (4)$$

and it follows immediately that for finite geometries (such as spheres, cubes, and finite cylinders)

$$\text{critical mass} = m_c \propto \rho^{-2}. \quad (5)$$

For the other two one-dimensional geometries, one can readily deduce that

$$\frac{\text{critical mass}}{\text{unit length of cylinder}} \propto \rho^{-1} \quad (6)$$

and

$$\frac{\text{critical mass}}{\text{unit area of slab}} \propto \rho^0 = \text{constant}. \quad (7)$$

This density law is general and is applicable to any mixture of materials in any geometrical shape and reflected in any manner provided only that the entire system be treated by the same factor throughout. The extrapolation distance also obeys this law.

An empirical and useful generalization applies to reflected systems in which one varies the density of the core and reflector independently. (23) For finite geometries the hypothesis is given a form comparable to that for bare systems. One asserts that

$$m_c \propto \rho_{\text{core}}^{-m} \rho_{\text{reflector}}^{-n} \quad (8)$$

and searches for those data which can provide values of  $m$  and  $n$ , subject to the boundary condition that  $m + n = 2.0$  (a lower limit for  $m$  is proposed in Section VIII B). Clearly these "constants" must be functions of the materials in the core and reflector, the reflector thickness, and, in some cases, the magnitudes of the densities. Considering the importance of changes of density in criticality physics, very little experimental and/or theoretical data are available. These few will be summarized.

Experimental data for metallic U(93.5) and  $\delta$ -phase plutonium reflected with varying thicknesses of normal uranium (23) suggest that, for this case,  $m$  is a function

of the degree of reflection. The experimental results can be summarized by the formula

$$m \approx 2.64 \frac{R_r}{R_b} - 0.64 \quad (9)$$

in which  $R_r$  and  $R_b$  are the reflected and bare critical radii, respectively. Errors in the exponent  $m$  as obtained from Eq. 9 seem to be random and less than  $\sim 10\%$ . The limit for the full-density U(93.5) core is  $m = 1.2$  (at  $R_r/R_b = 0.697$ ), and  $n$  is deduced to be 0.8 in order to harmonize with Eq. 5. Data, some of which led to Eq. 9, are illustrated by the two topmost curves of Fig. 2, in which the core is metallic plutonium with a reflector of natural uranium or thorium, and the core density exponent is illustrated as a function of reflector thickness. These data have not been examined theoretically.

For the more important nonmetal cores, data are equally scanty. Table III lists the known data for near equilateral cores of U(30), U(93), and plutonium compounds and mixtures with various reflectors.

The first four entries in Table III have been examined theoretically. Transformation of the parallelepipeds to spheres was accomplished by deducing a reflector

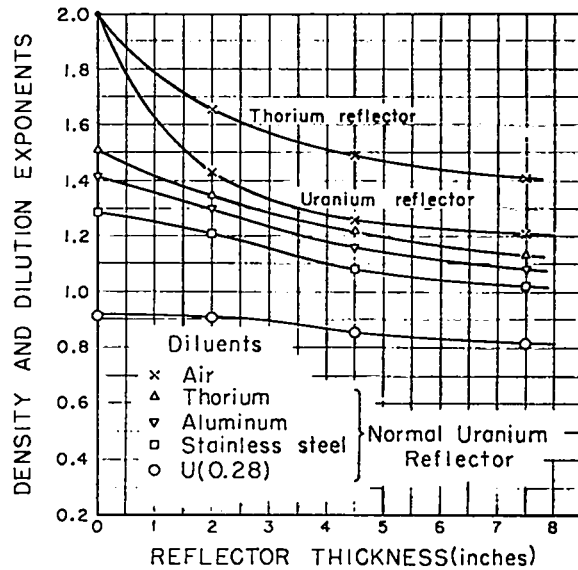


Fig. 2. Density and dilution exponents vs thickness of normal uranium reflector for plutonium metal cores mixed with several materials. The upper two curves are discussed in Section III while the lower four are considered in Section IV.

saving from unreflected experiments of the same composition and applying these results in Eq. 3. The theory predicts the critical radii of the transformed experiments to within  $\sim 2\%$ . The exponent itself, however, is an especially sensitive test as is sug-

TABLE III. DENSITY EXPONENT DATA

Core Material	$H/^{235}U$ or $H/^{239}Pu$	Reflector	Experimental m	Theoretical m	Reference
U(30)O <sub>2</sub> - Paraffin	8.26	lucite, 8 in.	1.55	1.544	24
"	16.5	"	1.55	1.530	"
"	16.5	polyethylene, 8 in.	1.687	1.632	"
"	81.8	"	1.764	1.644	"
U(93)O <sub>2</sub> NO <sub>3</sub> Solution	230.0	thick water	1.88	-	25
U(93)H <sub>3</sub> C	3.2	thick normal uranium	1.57	-	26
PuO <sub>2</sub> Polystyrene	15.0	lucite, 6 in.	1.50	-	27

gested by the table. It is not known why the calculations for polyethylene reflectors are less accurate than those for lucite reflectors.

Since density-exponent (or comparable) information is necessary for adequate treatment of experimental data, some calculations have been completed for Pu(100)-water,<sup>(13)</sup> U(93.5)-water,<sup>(13)</sup> U(93.5)-carbon-water,<sup>(28)</sup> U(30)-water, and U(5)-water cores, all reflected with ~20 cm water. These data are displayed in Fig. 3 as a function of the  $H/^{235}\text{U}$  or  $H/^{239}\text{Pu}$  atom ratio; the sundry exponents are derived from pairs of critical radius calculations in which the relative core density was changed from 1.0 (normal) to 0.8. For the U(93.5) metal ball in water, the density was reduced additionally in a series of calculations to as little as 1/10 normal with no change in the value of the exponent; for still lower densities, the exponent increased somewhat, suggesting that for very low densities its upper limit is

2.0 as in the unreflected core. It should be noted that very few of the data of Fig. 3 have been verified experimentally, and caution in application is advised.

In Sections VI and VII, detailed variable-density information on some graphite-moderated and graphite-reflected systems will be presented.

Experimental values for reflector density exponents seem nonexistent, yet quite necessary for an understanding of and use of critical data. In lieu of experimental data, calculations for three spherical U(93.5) metal-water mixture cores reflected with an essentially infinite water thickness\* (20 cm) have been completed. In these calculations, the water reflector density was reduced to 0.8 and 0.4 of normal water density while the reflector mass was held nearly constant. Reflector exponents ( $n$ ) for density changes of 1.0 to 0.8 and 0.8

\* Properly, the reflector thickness should be a constant number of mean free paths. This is practically the case for a thick (20-cm) water reflector.

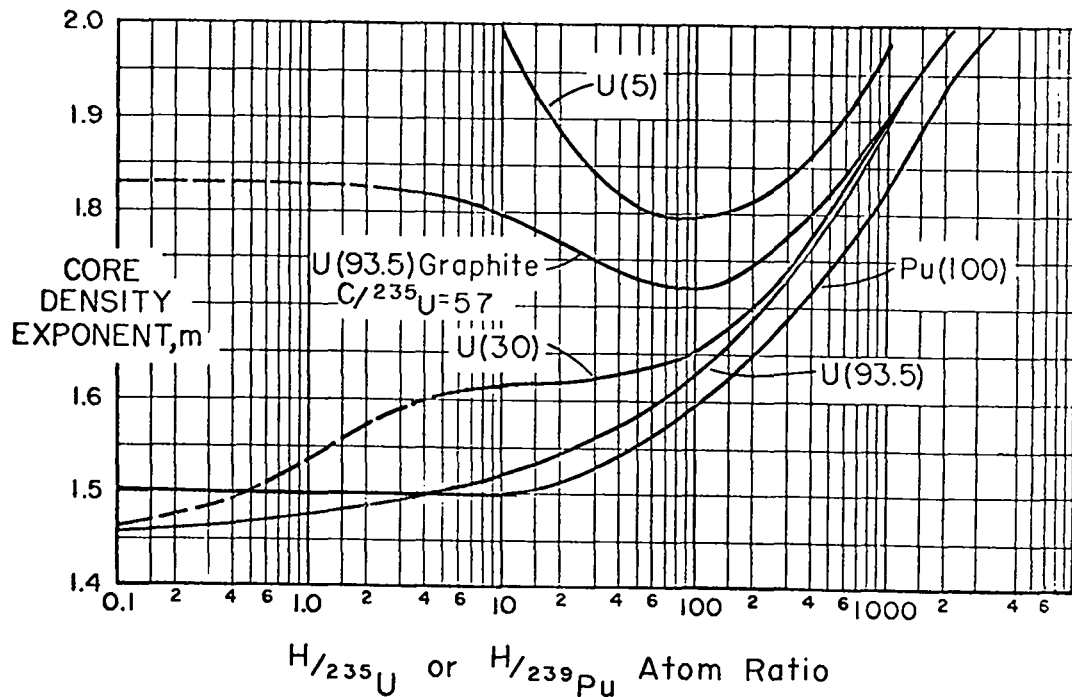


Fig. 3. Core density exponents for several materials vs the  $H/^{235}\text{U}$  or  $H/^{239}\text{Pu}$  atom ratio. The reflector is thick water at normal density in all cases.

to 0.4 are illustrated in Fig. 4 as a function of the  $H/^{235}U$  atom ratio of the core. The exponent for the latter change in density is less than that for the 1.0 to 0.8 shift, as expected, since a reflector density exponent must approach zero as a limit as the reflector becomes more and more tenuous. For the same  $H/^{235}U$  value and change in density, exponents  $m$  and  $n$  taken from Figs. 3 and 4 sum to 2.0 within 3%. Since this sum should be exactly 2.0 for only infinitesimal changes in density, this small deviation is regarded as unimportant.

IV. INTERNAL SCATTERING (DILUTION BY NON-MODERATORS)

Introduction of a limited amount of foreign material into a metal core invariably increases the critical mass, and for many medium to large  $Z$  elements, data can be generalized in terms of a constant "dilution" exponent, (18,23)  $p$ , defined by

$$m_c \propto \rho^{-p} \propto F^{-p} \quad (10)$$

In this equation  $\rho$  is the fissile material density, and  $F$  is the fraction of the core volume occupied by the fissile isotope. The introduction of a foreign material into a core can be imagined as taking place in two steps: first, the density is reduced, reducing criticality by creating some internal void space, and, to maintain the critical state, the mass must be increased as demanded by Eq. 5 or 8. Second, we imagine these internal voids to be filled with the foreign material; scattering from these atoms (internal reflection) tends to conserve some of the neutrons thus decreasing the critical mass below that allowed by density changes in Eq. 5 or 8. (Two exceptions exist for metal cores -- see Table IV.)

Considerable experimental information on dilution exponents for unreflected metal cores is available for values of  $F$  ranging from 1.0 to sometimes 0.3; these data (18, 29,30) are presented in Table IV.

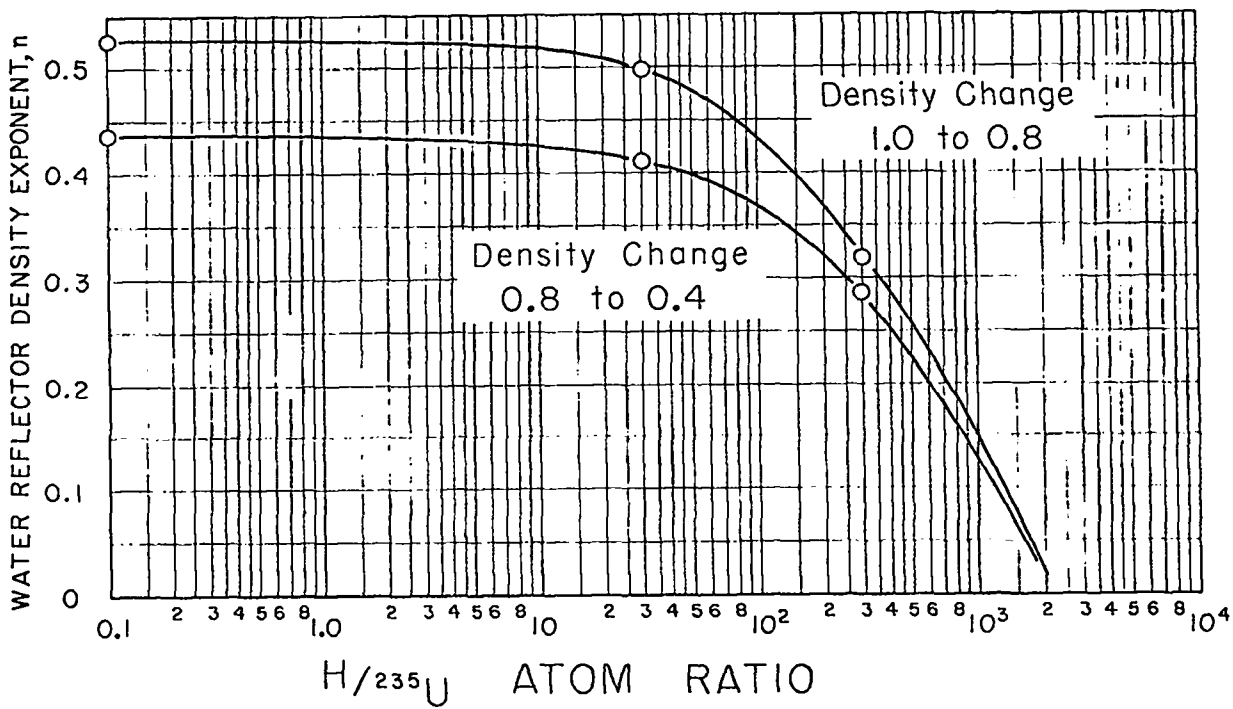


Fig. 4. Water reflector density exponents vs the core  $H/^{235}U$  atom ratio for water-reflected, water-moderated spheres. As the reflector exponent is dependent upon the magnitude of the reflector density, the function is illustrated for two changes of density.

TABLE IV. DILUTION EXPONENTS FOR UNREFLECTED METAL CORES

<u>Fissile Material</u>	<u>Diluent</u>	<u>p</u>	<u>Experimental Limit of F</u>
U(93)	${}^6\text{Li}$	2.31	~ 1.0
"	${}^{10}\text{B}$	2.93	~ 1.0
"	Carbon	1.097	0.45
"	Aluminum	1.31	0.43
"	Iron	1.19	0.38
"	Nickel	1.08	0.38
"	Copper	0.98	0.32
"	Zinc	1.16	0.38
"	Zirconium*	1.07	0.39
"	Hafnium	1.25	0.74
"	Tantalum	1.29	0.49
"	Tungsten	1.02	0.31
"	U(0.7)(normal)	0.7	0.30
Pu, $\delta$ phase	Aluminum(1100F)	1.51	0.52
"	Stainless Steel(304)	1.29	"
"	Thorium	1.42	"
"	U(0.28)	0.915	"

\*The data for zirconium seem to show linearity only for  $F < 0.8$  and seem to extrapolate to a critical mass value at  $F = 1$  of ~ 51.0 kg instead of 48 kg.

The unreflected critical mass of  ${}^{235}\text{U}$  diluted with  ${}^{238}\text{U}$  is known over an especially wide range.<sup>(18)</sup> Beyond the limit indicated in Table IV, the critical mass of  ${}^{235}\text{U}$  increases more rapidly as enrichment is decreased and becomes unbounded at an enrichment of between 5 and 6%. A similar behavior is expected for most of the diluents (except graphite and, perhaps, aluminum and zirconium) listed in Table IV, but experimental data are not available, and cross sections are probably not sufficiently accurate for quantitative predictions.

Some dilution information<sup>(3,18)</sup> for plutonium cores reflected with normal uranium is displayed in Fig. 2. The diluents here are thorium, aluminum, stainless steel, and depleted uranium, all of which seem to demand near-constant exponents for densities down to about one-half normal. As can be seen in Fig. 2, the exponent is very

slightly dependent on the reflector thickness. Similar data are available for thorium reflectors.

To my knowledge few, if any, of these data (except those for carbon and uranium diluents) have been correlated with theory.

Dilution exponents for a very large number of elements in fissile metal can be derived from reactivity coefficient data.<sup>(30)</sup> In these experiments a very small sample of the material of interest is substituted for the same volume of fissile material, and the change of reactivity is noted as a function of position in the core. The range of dilution over which these data can be trusted is quite limited.

To permit comparison of experimental and theoretical data and intercomparison experiments, the data must be reduced to common standards. The standards of shape were chosen to be spheres, slabs, and cyl-

inders. The standard for core composition also is arbitrary, and for those experiments performed with water solutions of the fissile-element salts such as fluorides and nitrates, the standard is a metal-water mixture. This standard has the advantages of simplicity (fewer components with which to contend) and of maximum density, hence minimum mass, for a given moderation and thus is conservative in terms of criticality safety. Of particular importance now are the diluting properties (displacement and neutron scattering and capturing) of oxygen, fluorine, etc., in the sundry water solutions used for experimental measurements. To reduce these experiments to the metal-water standard, the critical radius of the solution system is first calculated (allowing an exact comparison), and, second, the radius is again calculated, but without the atoms extraneous to the metal-water mixture (e.g., the  $O_2F_2$  in a  $UO_2F_2$  solution) and with the fissile element and water densities unchanged. To reduce this last value to a normal-density, metal-water system is now only a density conversion, which can be done with precision.

The increase in radius with removal of the internal scatterers depends upon the fissile atom density,  $H/^{235}U$  atom ratio, enrichment (of  $^{235}U$ ), reflector, and scattering atoms. This change in radius (defined to be the ratio of the radius without extraneous scattering atoms to the radius of the solution  $\bar{R}$ ) is illustrated in Fig. 5 for several applicable materials, but further generalization is possible. This ratio of radii is linear (for uranium systems) in the  $(^{235}U + ^{238}U)/H$  atom ratio, and can be expressed as

$$\bar{R} = \text{ratio of radii} = 1.0 + a(U/H). \quad (11)$$

For bare and reflected  $UO_2F_2$  solution systems, the constants are 1.156 and 0.784, while for  $UO_2(NO_3)_2$  the corresponding constants are 2.485 and 1.957, respectively.

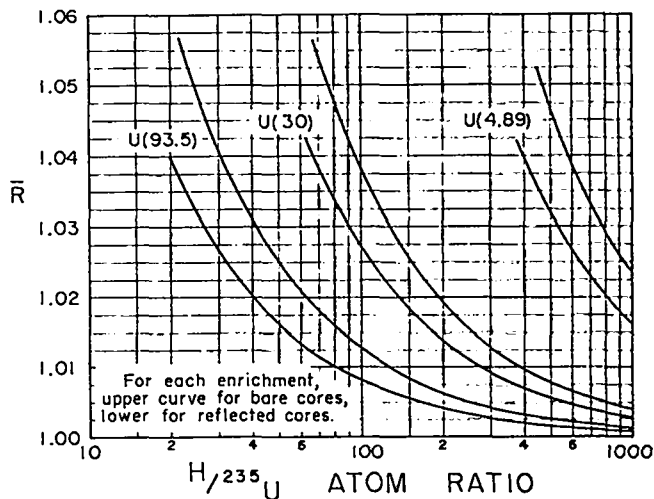


Fig. 5. Ratio ( $\bar{R}$ ) of uranium metal-water sphere radius to the  $UO_2F_2$  solution radius with densities appropriate to those of the solution vs the  $H/^{235}U$  atom ratio. This uranium density is invariably less than that for the ideal metal-water mixture.

These corrections have been used in the reduction of experimental data to standard conditions for comparison with theoretical results. The inverse is equally possible.

#### V. INTERNAL MODERATION (HYDROGEN, CARBON, AND OXYGEN)

If a neutron moderator (usually hydrogen, deuterium, beryllium, or carbon) is mixed with fissile metal, the initial effect is that of a diluent increasing the critical mass. However, the more important result of substantially reducing the neutron energy and thus increasing the spectrum-averaged fission cross section is also present, and with increasing volume fraction of moderating diluent the critical mass characteristically is reduced to a very low value. The penalty exacted for the decrease in fissile atom mass is a concomitant increase in critical volume -- the larger dimensions being required to accommodate the diluent necessary for moderation. As the volume fraction of moderator is increased without limit, the critical mass typically passes through a minimum



value ("full moderation") and thereafter increases rapidly and becomes unbounded at some asymptotic value of the fissile material density. A convenient and common measure of the degree of moderation is the moderator-atom/fissile-atom ratio (often written  $H/^{235}\text{U}$ ,  $C/\text{Pu}$ , etc.), and this ratio will be quoted in the tables that follow along with the fissile material densities and critical dimensions.

The theoretical data for U(93.5) cores will be presented as metal-graphite-water and oxide-water mixtures, while the data for U(30), U(5), U(3), U(2), U(1.42),  $^{239}\text{Pu}$ , and  $^{233}\text{U}$  will be given as metal-water mixtures with some cases including the oxide-water cores. The geometries will be one-dimensional, as defined, to be part of the standard presentation; but, in addition, the standard is taken to be the case in which any container about the core or between core and reflector is removed. Solution containers are generally fabricated of stainless steel or aluminum usually  $\sim 1/16$ -in. thick, but deviations are not uncommon. Where a comparison of theory and experiment is offered, the container or can is invariably imagined to be removed unless otherwise stated explicitly.

Rather thin containers of stainless steel can cause significant changes in the critical dimensions. Calculated corrections used for stainless steel for both bare and water-reflected systems are shown in Fig. 6 as a function of moderation, the  $H/^{235}\text{U}$  ratio. It should be noted that these curves are opposite in sign -- removal of stainless steel from between core and water reflector allows the core radius to decrease (stainless steel is a poison); removal from an otherwise bare core requires the core to become larger (stainless steel is a reflector). Aluminum is more innocuous; for bare systems  $1/16$  in. is worth about 0.05 cm on the sphere radius, while for water-reflected cores it is nearly invisible -- the corrections applied were 0.01, 0.02, 0.025,

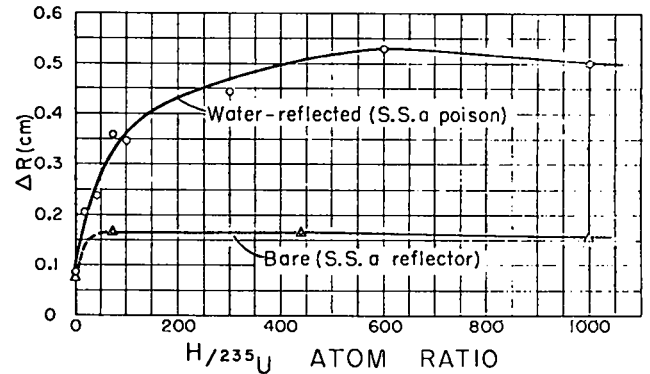


Fig. 6. Radius change for removal of a  $1/16$ -in. stainless steel container as a function of the  $H/^{235}\text{U}$  atom ratio.

0.02, and 0.01 cm at  $H/^{235}\text{U}$  values of 0, 40, 130, 280, and 400 and above. The sign for the aluminum correction is the same as that for the steel container. For different container thicknesses, these calculated corrections were scaled linearly.

Estimates of the accuracy of the theoretical results will be given by table or illustration for each isotope and each enrichment of  $^{235}\text{U}$ . The quality and number of experiments is quite different for each case, and generalizations as to overall accuracy will be avoided.

#### A. U(93.5) Metal-Water-Graphite and Oxide-Water Cores

The theoretical critical masses of spherical, unreflected mixtures of U(93.5) metal, water, and carbon<sup>(28)</sup> are illustrated in Fig. 7, and the critical dimensions of spheres, infinite slabs, and infinite cylinders composed of these mixtures, both bare and reflected with 20 cm of water, are given in Tables Va through Vj. Table Vk<sup>(31)</sup> contains the critical radii of bare and water-reflected mixtures of U(93.5) $\text{O}_2$ -water cores -- these radii differing from the metal-water values only for slightly moderated cores (low  $H/^{235}\text{U}$ ). In the preparation of these data, the " $\rho_0$ " or "crystal densities" of the materials were assumed to be 17.60 for  $^{235}\text{U}$  in U(93.5) metal, 8.93 for  $^{235}\text{U}$  in  $\text{UO}_2$ , 1.90 for graphite, and 1.0 for water, with mixture densities calculated

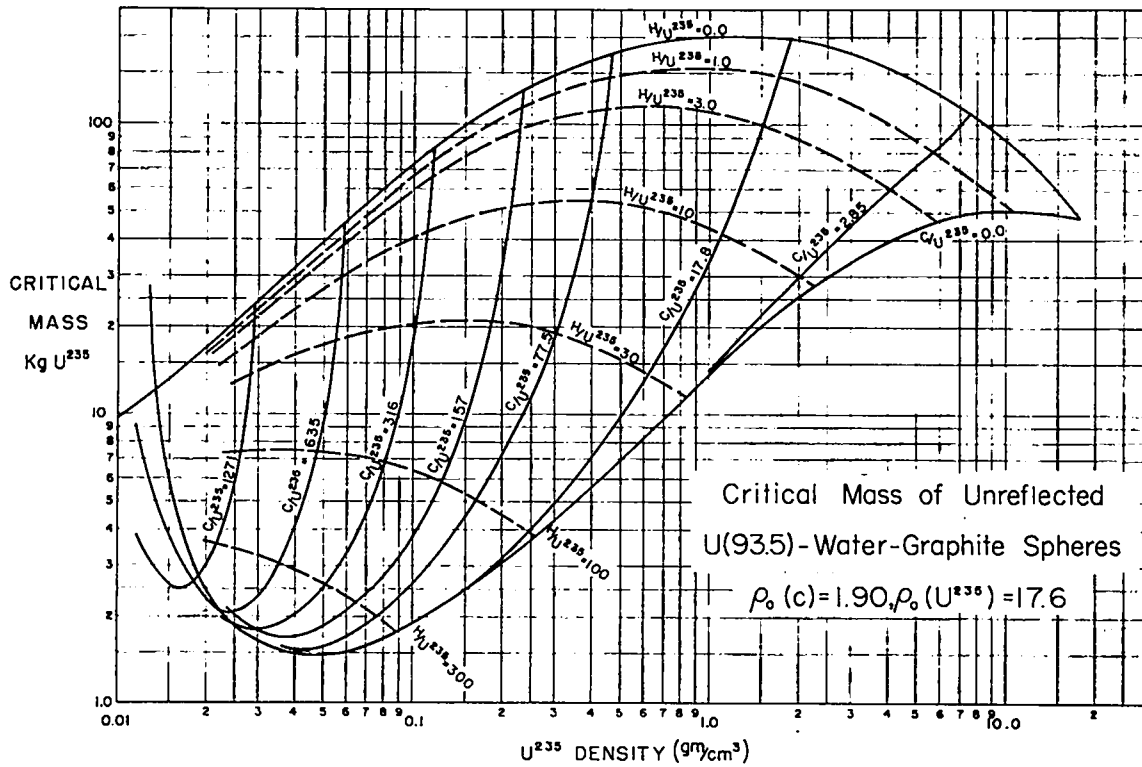


Fig. 7. Bare critical masses of the three-phase, U(93.5)-graphite-water system vs the  $^{235}\text{U}$  density. These data, all calculated values, are taken from Table V.

TABLE V. U(93.5) METAL-WATER-GRAPHITE MIXTURES  
Critical Dimensions for Slabs, Cylinders, and Spheres

$H/^{235}\text{U}$	$^{235}\text{U}$ Density ( $\text{g}/\text{cm}^3$ )	Unreflected			Water-Reflected		
		Slab Thickness (cm)	Cylinder Radius (cm)	Sphere Radius (cm)	Slab Thickness (cm)	Cylinder Radius (cm)	Sphere Radius (cm)
$v_a, C/^{235}\text{U} = 0.0$							
0.0	1.76 +1	6.862	6.104	8.652	1.757	3.845	6.636
1.00 +0	1.05 +1	8.541	7.461	10.447	2.382	4.694	8.110
3.00 +0	5.82 +0	10.347	8.911	12.382	3.184	5.972	9.250
9.96 +0	2.28 +0	12.202	10.368	14.323	4.142	6.574	10.685
1.72 +1	1.40 +0			14.679			10.952
3.00 +1	8.28 -1	12.736	10.752	14.805	4.723	6.898	11.058
1.00 +2	2.57 -1	13.220	11.087	15.206	5.580	7.391	11.522
3.00 +2	8.65 -2	14.989	12.437	16.978	7.798	8.896	13.431
5.20 +2	5.00 -2			19.167			15.751
1.00 +3	2.60 -2	23.292	18.895	25.451	16.458	15.459	21.989
1.50 +3	1.74 -2	34.297	27.451	36.581	27.502	23.961	33.086
2.00 +3	1.30 -2			75.445			

TABLE V (Continued)

$H/^{235}\text{U}$	$^{235}\text{U}$ Density ( $\text{g}/\text{cm}^3$ )	Unreflected			Water-Reflected		
		Slab Thickness (cm)	Cylinder Radius (cm)	Sphere Radius (cm)	Slab Thickness (cm)	Cylinder Radius (cm)	Sphere Radius (cm)
<u><math>V_b, C/^{235}\text{U} = 2.852</math></u>							
0.0	7.48 +0			15.143			11.349
1.80 -1	7.11 +0			15.022			
8.70 -1	5.98 +0			14.970			
2.33 +0	4.49 +0			15.104			
5.24 +0	2.99 +0			15.243			
3.14 +1	7.48 -1			14.689			
6.63 +1	3.74 -1			14.751			
<u><math>V_c, C/^{235}\text{U} = 17.774</math></u>							
0.0	1.87 +0			29.264			22.964
7.40 -1	1.78 +0			27.768			
3.49 +0	1.50 +0			24.569			
9.31 +0	1.12 +0			21.113			
2.09 +1	7.48 -1			18.145			
5.58 +1	3.74 -1			16.001			
1.85 +2	1.31 -1			16.044			
<u><math>V_d, C/^{235}\text{U} = 77.46</math></u>							
0.0	4.68 -1	42.261	33.544	44.720	24.135	24.849	35.727
5.60 -1	4.63 -1			42.798			34.923
2.94 +0	4.44 -1	37.442	29.857	39.845	20.780	21.472	31.328
1.40 +1	3.74 -1	27.656	22.302	29.938	13.775	15.395	22.903
3.72 +1	2.81 -1	21.043	17.161	23.209	9.638	11.556	18.028
2.23 +2	9.35 -2	16.435	13.503	18.372	8.335	9.489	14.351
6.42 +2	3.74 -2	19.599	15.920	21.536	12.170	12.392	18.053
1.30 +3	1.93 -2						28.867
1.81 +3	1.40 -2						51.393
<u><math>V_e, C/^{235}\text{U} = 157</math></u>							
0.0	2.34 -1	19.120	38.778	51.184	29.418	28.886	41.663
1.13 +0	2.31 -1			49.498			40.120
5.88 +0	2.22 -1	40.859	32.456	43.249	23.322	23.667	34.304
2.79 +1	1.87 -1	28.429	22.859	30.767	14.817	15.885	23.737
7.45 +1	1.40 -1	21.685	17.629	23.863	10.628	12.147	18.539
2.07 +2	8.18 -2						15.923
4.47 +2	4.68 -2	18.919	15.382	20.840	11.213	11.436	16.942
9.04 +2	2.57 -2						21.960
1.30 +3	1.85 -2						29.801
1.75 +3	1.40 -2	47.290	37.420	48.885	42.154	34.594	45.860

TABLE V (Continued)

$C/^{235}\text{U}$	$^{235}\text{U}$ Density ( $\text{g}/\text{cm}^3$ )	Unreflected			Water-Reflected		
		Slab Thickness (cm)	Cylinder Radius (cm)	Sphere Radius (cm)	Slab Thickness (cm)	Cylinder Radius (cm)	Sphere Radius (cm)
$V_f, C/^{235}\text{U} = 316.2$							
0.0	1.17 -1	53.324	41.977	55.455	33.062	28.886	45.412
2.26 +0	1.16 -1			52.776			42.897
1.10 +1	1.11 -1	42.280	33.510	44.470	25.192	23.667	35.609
5.58 +1	9.35 -2	29.169	23.405	31.436	15.903	15.885	24.431
1.49 +2	7.01 -2	22.889	18.529	25.020	12.250	12.147	19.630
3.35 +2	4.68 -2	20.852	16.914	22.829	12.889	11.436	18.301
8.93 +2	2.34 -2	24.967	20.062	27.047	17.037	34.594	24.003
1.30 +3	1.71 -2						31.191
$V_g, C/^{235}\text{U} = 634.5$							
0.0	5.84 -2	54.914	43.180	57.214	34.919	32.974	47.903
2.35 +1	5.55 -2	43.094	34.080	45.343	26.090	25.140	35.920
1.12 +2	4.68 -2	30.547	24.444	32.718	17.665	17.803	25.925
2.98 +2	3.51 -2	25.321	20.370	27.384	15.302	15.136	22.256
6.70 +2	2.34 -2	25.645	20.593	27.638	17.254	16.204	23.527
1.79 +2	1.17 -2	54.693	43.079	57.111	46.120	40.026	55.492
$V_h, C/^{235}\text{U} = 1271$							
0.0	2.92 -2	55.897	43.841	58.192	36.395	33.540	48.800
4.70 +1	2.78 -2	44.537	35.164	46.715	28.097	26.812	36.859
2.23 +2	2.34 -2	33.326	26.523	35.457	21.193	20.210	29.031
5.96 +2	1.75 -2	30.587	24.399	32.630	20.988	19.378	27.455
1.34 +2	1.17 -2	40.453	32.026	42.653	33.100	27.382	39.531
$V_i, C/^{235}\text{U} = 5091$							
0.0	7.30 -3			63.524			
3.61 +1	7.23 -3			61.258			
1.88 +2	6.94 -3			55.121			
3.97 +2	6.57 -3			52.227			
8.94 +2	5.84 -3			54.196			
1.53 +3	5.11 -3			72.323			
$V_j, H/^{235}\text{U} = 0$							
0.0	1.76 +1			8.652			6.636
9.40 -1	1.22 +1			11.220			
2.85 +0	7.48 +0			15.143			11.349
7.83 +0	3.74 +0			21.804			
1.78 +1	1.87 +0			29.264			22.964
3.77 +1	9.35 -1			36.999			
7.75 +1	4.68 -1			44.720			35.727
1.57 +2	2.34 -1			51.184			41.663
3.16 +2	1.17 -1			55.455			45.412

TABLE V (Continued)

$C/^{235}\text{U}$	$^{235}\text{U}$ Density (g/cm <sup>3</sup> )	Unreflected			Water-Reflected		
		Slab Thickness (cm)	Cylinder Radius (cm)	Sphere Radius (cm)	Slab Thickness (cm)	Cylinder Radius (cm)	Sphere Radius (cm)
$V_j, H/^{235}\text{U} = 0$ (Continued)							
6.35 +2	5.84 -2			57.214			47.903
1.27 +3	2.92 -2			58.192			48.800
2.54 +3	1.46 -2			59.728			
5.09 +3	7.30 -3			63.524			53.139
1.02 +4	3.65 -3			70.751			
2.04 +4	1.83 -3			83.006			
4.07 +4	9.13 -4			105.500			
8.15 +4	4.57 -4			152.900			
1.63 +5	2.28 -4			425.600			

Vk, U(93.5)O<sub>2</sub> METAL OXIDE-WATER MIXTURES

$H/^{235}\text{U}$	Density (g/cm <sup>3</sup> )	Unreflected			Water-Reflected		
		Slab Thickness (cm)	Cylinder Radius (cm)	Sphere Radius (cm)	Slab Thickness (cm)	Cylinder Radius (cm)	Sphere Radius (cm)
0.0	8.93 +0	11.35	9.69	13.43	3.748	6.21	10.63
9.80 -1	6.70 +0	11.86	10.06	13.90	3.990	6.49	10.49
2.94 +0	4.47 +0	12.78	10.78	14.87	4.549	7.00	11.14
8.96 +0	2.23 +0	13.74	11.53	15.85	5.114	7.51	11.75
2.06 +1	1.12 +0	13.55	11.34	15.60	5.098	7.34	11.53
4.39 +1	5.58 -1	13.32	11.13	15.27	5.197	7.22	11.39

on a simple volume displacement scheme. Tables Va and Vj provide the envelope for the family of curves of Fig. 7 -- the numbers in Table Va are the well-known critical data for mixtures of enriched uranium and water, while the data of Table Vj are comparable with graphite replacing water -- the table extends the data beyond the range illustrated in Fig. 7. In this and the following tables, densities and atom ratios are presented in a condensed notation, e.g.,  $3.14 \times 10^5 \equiv 3.14 + 5$ ,  $6.2 \times 10^{-5} \equiv 6.2 - 5$ .

Of particular interest is the tremendous moderating power of water when it is added to a graphite-U(93.5) mixture which has a  $C/^{235}\text{U}$  atom ratio of, for example,  $\lambda > 70$  -- the critical mass drops precipitously with the addition of small amounts of

water. Conversely, some preliminary results (not included) for which  $C/^{235}\text{U} \sim 2 \times 10^4$  suggest that hydrogen is invariably a poison when mixed in the form of water with this fully moderated material. Also from Fig. 7, the possibility of obtaining dilution exponents for graphite in various U(93.5) metal-water mixtures is evident.

For the U(93.5)-water systems, the relationship between  $^{235}\text{U}$  density and  $H/^{235}\text{U}$  atom ratio is

$$\rho(^{235}\text{U}) = \frac{26.082}{1.483 + H/^{235}\text{U}} ; \quad (12)$$

the comparable relationship for the U(93.5)-graphite systems is

$$\rho(^{235}\text{U}) = \frac{37.176}{2.112 + C/^{235}\text{U}} . \quad (13)$$

Comparison with experimental data to justify presenting these computational results as fact will be presented in Figs. 8 and 9 and in the discussion below. The experiments validating the U(93.5)-graphite data (the uppermost curve of Fig. 7) were performed with thin metal plates interleaved between slabs of graphite.<sup>(32)</sup> Differences between theory and experiment are trivial (0.5 to 1% on the radius for 14 points) except for one point at  $\rho(^{235}\text{U}) = 0.52 \text{ g/cm}^3$  where the calculated radius is 3% higher than the experimental value. In addition to these data, experiments at  $C/^{235}\text{U}$  ratios of about 300, 600, 1300, 2500, and 10,000 indicate that<sup>(18,33-35)</sup> in this better-moderated region the theory is good to ~1% on the radius. Thus the unreflected U(93.5)-graphite data may be accepted as accurate to within ~1% on a dimension (3% on mass).

Data from precise water- (or other hydrogenous) reflected U(93.5)-graphite experiments are not available.

Data pertinent to the lower limiting curve ( $C/^{235}\text{U} = 0$ ) of Fig. 7 are found in Figs. 8 and 9. Figure 8 shows, on a grossly expanded scale, critical radii for spherical systems whose  $^{235}\text{U}$  densities are between 1.0 and 0.07  $\text{g/cm}^3$ . For this region, because of the very large number of experimental points<sup>(36-45)</sup> and because of the interesting minimum in size at  $\rho(^{235}\text{U}) \sim 0.45 \text{ g/cm}^3$ , the comparison is made with the core assumed to be a  $\text{UO}_2\text{F}_2$  solution instead of a metal-water mixture (metal-water critical dimensions increase monotonically with increasing moderation). Uranyl nitrate solution dimensions were converted to those for fluoride, and, in all cases, the containers were imagined to be removed. Several points

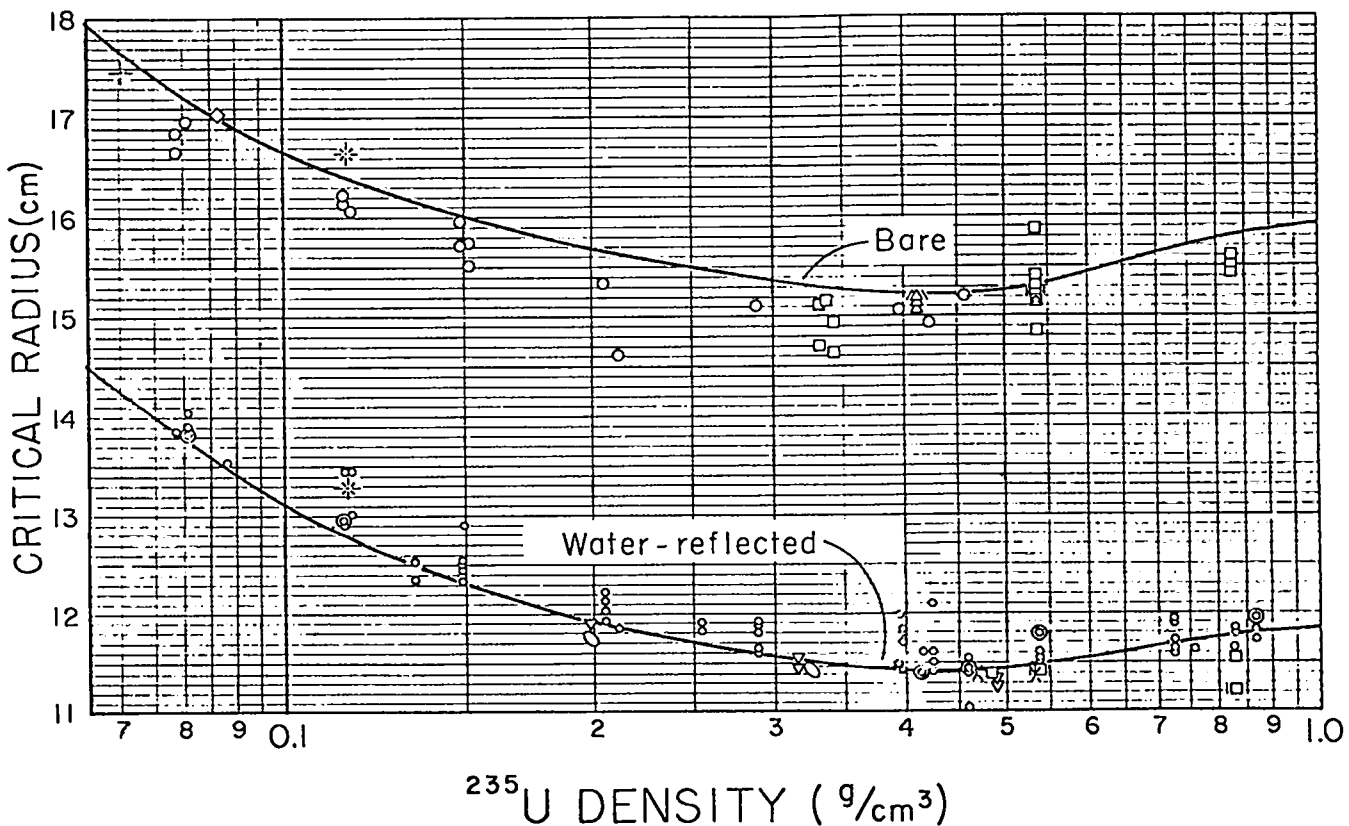


Fig. 8. Critical radii of  $\text{U}(93.5)\text{O}_2\text{F}_2$  water solutions, bare and water-reflected, vs  $^{235}\text{U}$  density. The solid lines derive from calculations. The experimental points here and in Fig. 9 derive from many different laboratories; symbols and references are:  $\circ$ , 36;  $\square$ , 37;  $\nabla$ , 38;  $\circ$ , 39;  $\times$ , 40;  $\triangle$ , 41;  $\circ$ , 42;  $+$ , 43;  $\diamond$ , 44;  $*$ , 45.

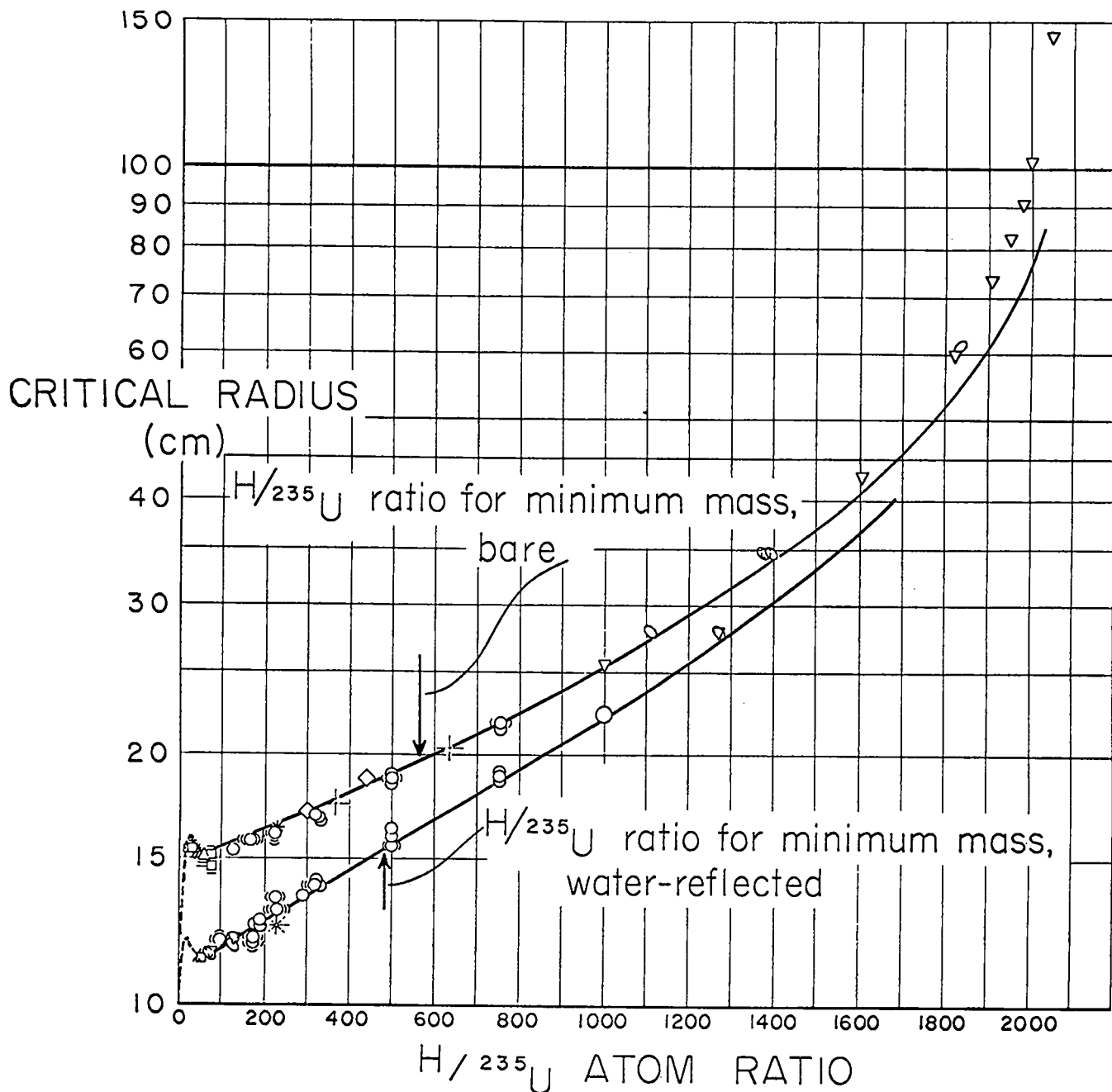


Fig. 9. Critical radii of  $U(93.5)O_2F_2$  water solutions, bare and water-reflected, vs the  $H/^{235}U$  atom ratio. The solid line represents the results of theory. Symbols are defined in the caption for Fig. 8.

at the same density imply experiments using the same solution but performed in containers of differing shape, usually of cylinder height-to-diameter ratios. These dimensions were converted to sphere radii using the schemes developed in Section II, and, apparently, the general question of shape conversion is not fully resolved.

In some respects the  $^{235}U$  density region of Fig. 8 suffers from a plethora of data. Some of the earlier results have been questioned, but fluctuations in radii seem to average no worse than those from some of the more modern experiments. Without more justification than mere age, data should not be discarded.

In this range of  $^{235}\text{U}$  density and  $\text{H}/^{235}\text{U}$  atom ratio, any estimate of error or deviation of theory from experiment must derive from Fig. 8. This is difficult, but for the unreflected systems, general agreement would be better if the theory predicted radii to be  $\sim 1\%$  lower (3% in mass). In contrast, the predicted radii for the water-reflected cores seem to be in good agreement for  $^{235}\text{U}$  densities greater than  $\sim 0.45 \text{ g/cm}^3$ , and average  $\sim 1\%$  low for the lower density region. I note that experiments may have suffered some difficulties near the limit of  $\text{UO}_2\text{F}_2$  solution solubility ( $^{235}\text{U}$  density  $\sim 1.0$ ).

Figure 9 presents the complete moderation range, but emphasizes the very low  $\text{U}(93.5)$  density water-moderated data in which critical radii of solution spheres are plotted as a function of  $\text{H}/^{235}\text{U}$  atom ratio. The dense clustering of experimental points for which  $\text{H}/^{235}\text{U} \lesssim 200$  is shown only in part as these data are more adequately displayed on Fig. 8. In general, agreement is satisfactory for  $\text{H}/^{235}\text{U} < 1200$ ; for greater moderation the theory predicts radii lower than those found by experiment. Interestingly, the limiting asymptote,  $k_\infty = 1.0$ , is calculated to be at an  $\text{H}/^{235}\text{U}$  atom ratio of 2220.0 ( $^{235}\text{U}$  density =  $11.74 \times 10^{-3} \text{ g/cm}^3$ ), while an extrapolation of critical solution data<sup>(18)</sup> to zero buckling gives  $\text{H}/^{235}\text{U} = 2136$  and  $\rho(^{235}\text{U}) = 12.2 \times 10^{-3} \text{ g/cm}^3$ . A recent experiment<sup>(46)</sup> places the  $^{235}\text{U}$  density at  $12.05 \pm 0.03 \text{ g/cm}^3$  for  $k_\infty = 1.0$ .

The critical values<sup>(3)</sup> for the end points of full metal density are mentioned in Section I; theory and experiment are in satisfactory agreement. The range of moderation for  $0 \leq \text{H}/^{235}\text{U} \lesssim 35$  and for several values of  $\text{C}/^{235}\text{U}$  has been studied recently, and some preliminary results<sup>(46)</sup> are available. Critical data were obtained by stacking  $\text{U}(93.5)$  foil ( $\sim 2 \times 10^{-3}$  to  $12 \times 10^{-3}$  in.-thick) with layers of lucite and graphite in an aluminum matrix, the unit of which

was a square, thin-walled tube, 3 x 3 in. in cross section. The relative amounts of foil, lucite, and graphite were varied to obtain different values of the two atom ratios, and for several moderation ratios, foil thicknesses were changed while holding the atom ratios constant, to provide a means of extrapolation to the homogeneous case. Most of these assemblies were parallelepipedal in shape, and a transformation to spheres was necessary; the transformed dimensions, atomic ratios, and theoretical results are shown in Table VI. Some of the points derive from several experiments, and in these cases the spread is no more than 1 or 2%. As can be seen in Table VI, the calculation seems to predict the experiments most satisfactorily. Because of these experiments the calculated dimensions applying to the slightly moderated systems of Table V may, for the first time, be accepted as representing reality in a precise manner.

Critical data calculated for  $\text{U}(93.2)$  moderated and reflected by polyethylene, lucite, and water<sup>(13)</sup> have been published, but are not reproduced here. Because of its greater hydrogen density, polyethylene allows the smallest critical mass for a given  $^{235}\text{U}$  density.

#### B. Uranium Enriched to Thirty Percent, U(30)

The critical parameters of  $\text{U}(30)$  metal-water mixtures are listed for both the bare and water-reflected cores in Table VII, while Fig. 10 contains a comparison of theory and experiment<sup>(24,43)</sup> for this enrichment. The experiments, except for the metal point,<sup>(3)</sup> are either  $\text{UO}_2\text{F}_2$  water solutions (spheres and finite cylinders) or parallelepipeds composed of mixtures of  $\text{UO}_2$  powder and paraffin.

The solution data<sup>(43)</sup> have been converted to metal-water spheres (using the schemes developed in Sections II and IV), and the dimensions adjusted for the removal of the container (Section IV) -- either



TABLE VI. FOIL, LUCITE, AND GRAPHITE LAMINAE

Bare and Lucite-Reflected

$H/^{235}\text{U}$	$C/^{235}\text{U}$	$\rho(^{235}\text{U})$ ( $\text{g}/\text{cm}^3$ )	Reflector	Experimental Radius (cm)	Theoretical Radius (cm)	$\frac{R_{\text{DTK}}}{R_{\text{Exp}}}$
5.99 +0	3.74 +0	2.12 +0	none	18.367	18.435	1.004
1.21 +1	7.57 +0	1.32 +0	none	18.763	18.841	1.004
1.23 +1	9.81 +1	2.58 -1	none	39.532	39.853	1.008
3.54 +1	2.21 +1	4.77 -1	none	19.132	19.238	1.006
3.52 +1	4.81 +1	3.38 -1	none	23.096	23.210	1.005
3.50 +1	1.02 +2	2.24 -1	none	27.243	27.589	1.013
1.22 +1	7.60 +0	1.31 +0	lucite, 8 in.	13.468	13.406	0.995
1.21 +1	1.01 +2	2.50 -1	lucite, 8 in.	34.130	33.484	0.981

TABLE VII. U(30) METAL-WATER MIXTURES

Critical Dimensions for Slabs, Cylinders, and Spheres

$H/^{235}\text{U}$	$^{235}\text{U}$ Density ( $\text{g}/\text{cm}^3$ )	Unreflected			Water-Reflected		
		Slab Thickness (cm)	Cylinder Radius (cm)	Sphere Radius (cm)	Slab Thickness (cm)	Cylinder Radius (cm)	Sphere Radius (cm)
0.0	5.69 +0	14.524	12.210	16.720	4.948	7.746	12.525
1.00 +0	4.67 +0	14.278	11.978	16.386	5.118	7.751	12.417
3.00 +0	3.44 +0	14.516	12.163	16.636	5.436	7.953	12.649
1.00 +1	1.79 +0	15.422	12.882	17.602	6.060	8.498	13.349
3.00 +1	7.54 -1	14.986	12.525	17.131	6.036	8.252	12.948
7.40 +1	3.32 -1			16.608			12.663
1.00 +2	2.49 -1	14.550	12.139	16.595	6.424	8.208	12.732
3.00 +2	8.56 -2	15.856	13.130	17.864	8.376	9.476	14.279
4.40 +2	5.87 -2			19.214			
6.00 +2	4.31 -2	18.894	15.473	20.946	11.712	11.947	17.461
1.00 +3	2.60 -2	24.390	19.730	26.570	17.366	16.286	23.121
1.50 +3	1.73 -2	36.562	29.109	39.185	29.654	25.751	35.529

stainless steel or aluminum. In general, except for one set of unreflected data near  $\rho(^{235}\text{U}) \sim 0.3$  (these had aluminum containers), the agreement between theory and experiment for the range illustrated is good. For the more dilute systems (low  $^{235}\text{U}$  density and large  $H/^{235}\text{U}$ , not illustrated) the theory seems to underestimate critical radii, as was the case for U(93.5). At  $H/^{235}\text{U} = 1000$ , the calculation is excellent, but

at dilutions of  $H/^{235}\text{U} \sim 1500$ , the theory is low by about 8% on the radius. Data for the limiting asymptote are not available.

The  $\text{UO}_2$ -paraffin experiments<sup>(24)</sup> were transformed to spheres using the scheme of Section II and reflector savings derived from the experiments. In this case, core mixture transformations were not attempted -- the actual atom densities were inserted into the code, radii were calculated, and

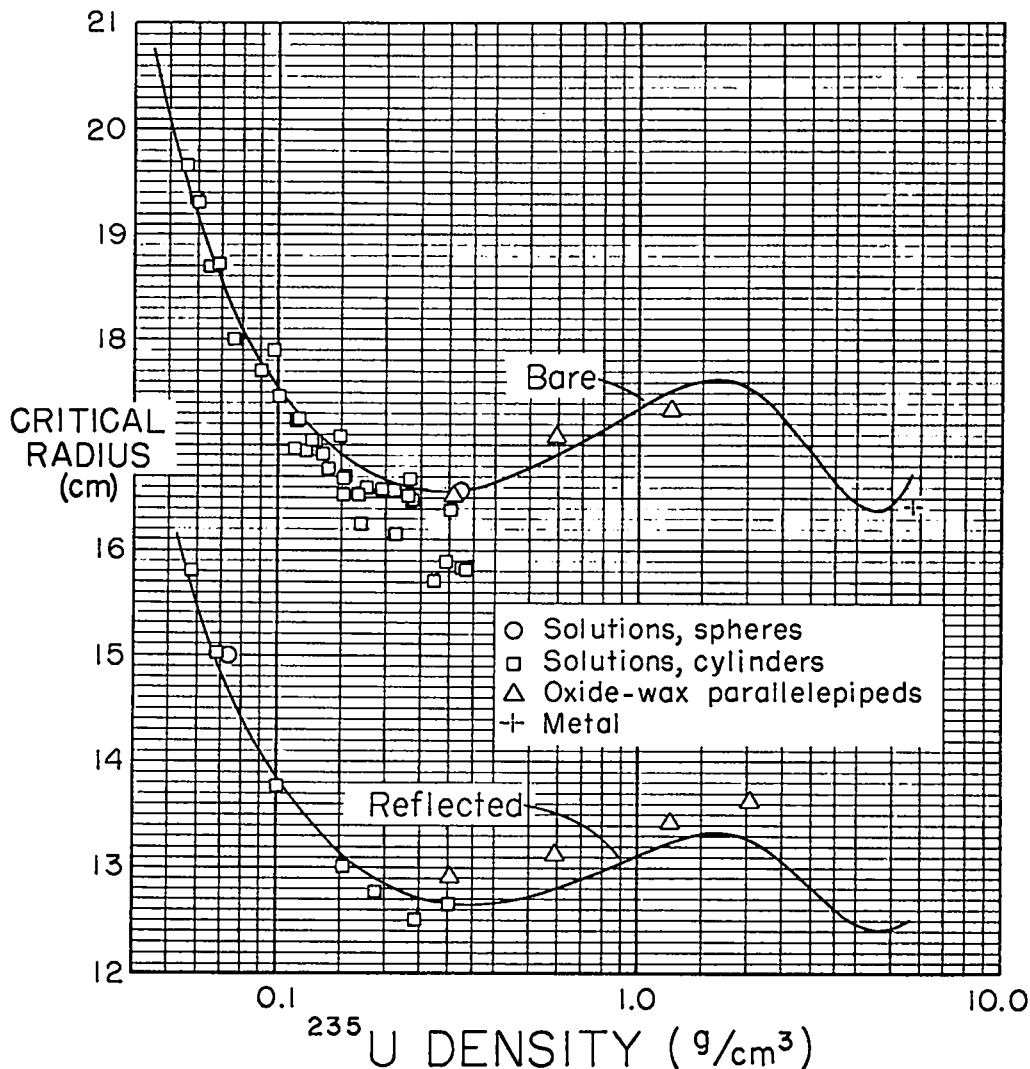


Fig. 10. Critical radii for U(30) metal-water cores, bare and water-reflected, vs <sup>235</sup>U densities.

deviations from experiment were noted. The points plotted on Fig. 10 represent metal-water mixtures and are in the same ratio to the theoretical radii as were the actual experiments and calculations -- the ability of a theory to predict a radius for a U(30)O<sub>2</sub>-paraffin system implies equally the ability to calculate a U(30) metal-water system. The H/<sup>235</sup>U atom ratios for these experiments were 8.26, 16.53, 40.0, and 81.8. Deviations of theory from experiment seem to be less than ~2.5% on radius, the calculations usually, but not always, being low.

These data contain the set that allowed a deduction of some core density exponents in Section III, Table III. For these experiments, the core density was reduced by about 1/3, and additional core material was then added to regain the critical state.

Precise experiments with enriched uranium systems only slightly diluted and moderated by hydrogen are rare, and these experiments at H/<sup>235</sup>U atom ratios of 8.26 and 16.53 are most useful. These data and the low H/<sup>235</sup>U U(93.5)-lucite experimental data complement each other and give added credence to theoretical predictions of criti-

cal parameters in this range of moderation.

For U(30) metal-water mixtures, the relationship between fissile metal density and moderation is

$$\rho(^{235}\text{U}) = \frac{26.082}{4.5811 + H/^{235}\text{U}} \quad (14)$$

### C. Uranium Enriched to Five Percent, U(5)

In Section IV it was noted that as highly enriched uranium is progressively diluted with  $^{238}\text{U}$ , the critical geometry steadily increases and becomes unbounded for systems whose enrichments lie between 5 and 6 wt%  $^{235}\text{U}$ . Thus, homogeneous uranium systems of such low enrichment cannot be made critical without the addition of a third material, a moderator, and we have now qualitative as well as quantitative differences between the criticality physics of highly and poorly enriched systems. These poorly enriched systems show a true minimum in a plot of any critical parameter versus  $^{235}\text{U}$  density or  $H/^{235}\text{U}$  atom ratio and show two asymptotes, at low and high moderation, whereas the highly enriched metal-water mixtures show a minimum only for the critical mass, and one asymptote at high moderation.

Table VIIIa contains the calculated values of the critical parameters for U(5) metal-water systems, while Table VIIIb shows the same data, bare and water-reflected, for U(5) $\text{O}_2$ -water mixtures.<sup>(31)</sup> Some of these same data (sphere radii) are displayed on Fig. 11 as a function of the  $^{235}\text{U}$  density. The minimum critical volume for the metal-water systems occurs at a density of  $0.1 \text{ g/cm}^3$ , while the effect of the oxide on the minimum is to cause a shift to  $0.085 \text{ g/cm}^3$ . The minimum critical mass, however, is found at a substantially lower density. This value is  $0.05 \text{ g/cm}^3$  for the metal-water and  $0.04 \text{ g/cm}^3$  for the oxide-water cores. The relationship between  $^{235}\text{U}$  density and  $H/^{235}\text{U}$  atom ratio for U(5) metal-water is

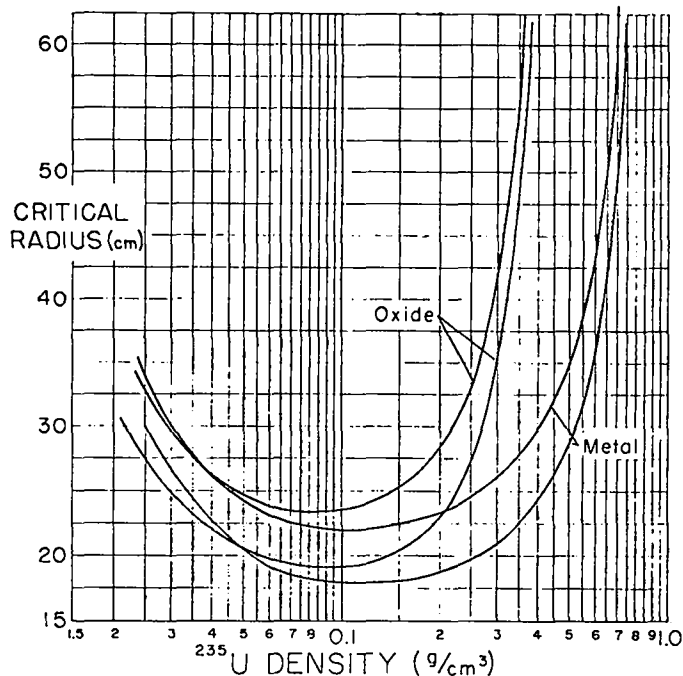


Fig. 11. Theoretical critical radii for U(5) metal-water and U(5) $\text{O}_2$ -water spheres vs  $^{235}\text{U}$  density. Direct comparison to experiments for this enrichment is in Tables IX and X.

$$\rho(^{235}\text{U}) = \frac{26.082}{27.40 + H/^{235}\text{U}} \quad (15)$$

The experimental data<sup>(47)</sup> pertinent to this enrichment come from two sets of experiments. The first is the steadfast  $\text{UO}_2\text{F}_2$ -water solution, bare and water-reflected. The enrichment is 4.89%, sufficiently close to the 5% of Table VIII for comparison. These data, each point of which represents several experiments, are displayed in Table IX in which a comparison (ratio of calculated to experimental radius) to theory is also offered. A trend may be anticipated here -- for the bare systems, the theory is 2.2% high for low  $H/^{235}\text{U}$  ratios but 1% low for high  $H/^{235}\text{U}$  ratios. For water-reflected systems, the theory seems to be excellent for  $H/^{235}\text{U} = 524$  but 2.6% low for  $H/^{235}\text{U} = 1025$ .

The second set of data<sup>(47)</sup> were obtained by use of mixtures of  $\text{U}(4.89)_3\text{O}_8$  and Sterotex, a glycerol tristearate,

TABLE VIIIa. U(5) METAL-WATER MIXTURES

Critical Dimensions for Slabs, Cylinders, and Spheres

$H/^{235}\text{U}$	$^{235}\text{U}$ Density ( $\text{g}/\text{cm}^3$ )	Unreflected			Water-Reflected		
		Slab Thickness (cm)	Cylinder Radius (cm)	Sphere Radius (cm)	Slab Thickness (cm)	Cylinder Radius (cm)	Sphere Radius (cm)
1.00 +1	6.98 -1	55.428	43.621	58.05	38.666	35.608	49.56
2.00 +1	5.51 -1	36.114	28.820	38.51	22.280	22.162	31.75
5.00 +1	3.37 -1	25.068	20.319	27.41	14.004	14.970	22.01
1.00 +2	2.05 -1	21.218	17.336	23.49	11.610	12.673	18.78
2.00 +2	1.15 -1	19.938	16.337	22.16	11.308	12.124	17.91
4.00 +2	6.11 -1	20.786	16.980	23.00	12.878	13.097	19.04
6.00 +2	4.16 -1	23.942	19.415	26.18	16.348	15.678	22.42
9.00 +2	2.81 -1	28.902	23.265	31.12	21.290	19.593	27.50

TABLE VIIIb. U(5)O<sub>2</sub> METAL OXIDE-WATER MIXTURES

Critical Dimensions for Slabs, Cylinders, and Spheres

$H/^{235}\text{U}$	$^{235}\text{U}$ Density ( $\text{g}/\text{cm}^3$ )	Unreflected			Water-Reflected		
		Slab Thickness (cm)	Cylinder Radius (cm)	Sphere Radius (cm)	Slab Thickness (cm)	Cylinder Radius (cm)	Sphere Radius (cm)
1.10 +1	3.97 -1						94.73
1.50 +1	3.75 -1			70.08			
1.83 +1	3.58 -1						51.28
2.50 +1	3.28 -1			48.04			
5.00 +1	2.49 -1			32.92			
5.49 +1	2.39 -1						25.98
1.00 +2	1.69 -1			26.17			
1.67 +2	1.19 -1						19.47
2.00 +2	1.03 -1			23.63			
3.91 +2	5.97 -2						19.91
4.00 +2	5.74 -2			24.00			
6.00 +2	3.99 -2			26.20			
7.84 +2	2.99 -2						24.95
9.00 +2	2.73 -2			31.03			

TABLE IX. U(4.89)O<sub>2</sub>F<sub>2</sub> WATER SOLUTIONS

$H/^{235}\text{U}$	$\rho(^{235}\text{U})$ ( $\text{g}/\text{cm}^3$ )	Unreflected			Water-Reflected		
		Radius		Ratio	Radius		Ratio
		Exp (cm)	Theory (cm)		Exp (cm)	Theory (cm)	
5.24 +2	4.25 -2	25.69	26.26	1.022	22.42	22.41	1.0
6.43 +2	3.56 -2	27.11	27.65	1.020	23.77	23.89	1.005
7.35 +2	3.18 -2	28.58	28.87	1.010	25.28	25.17	0.996
1.03 +3	2.35 -2	35.09	34.73	0.99	31.98	31.14	0.974

$(C_{17}H_{35}COO)_3C_3H_5$ , density  $0.862 \text{ g/cm}^3$ , with a molecular weight of 891.5. The density of hydrogen in Sterotex is  $0.1072 \text{ g/cm}^3$ , comparable to that of water. This mixture was packaged in thin-walled (1/16 in.) aluminum boxes whose outside dimensions, in inches, were  $8 \times 8 \times 8$ ,  $8 \times 8 \times 4$ , and  $4 \times 4 \times 4$ . Thus all experiments were parallel-pipedal in shape, and a conversion to spherical geometry was required. Even though the extrapolation distances are poorly known ( $\delta$  assumed to be 2.5 cm, and observed  $\Delta R$ 's were used), the errors from this source are probably small compared to the estimated average experimental error of  $\pm 2\%$  on the radius.

In Table X, experimental and theoretical radii and their ratios are presented along with pertinent  $H/^{235}\text{U}$  ratios and  $^{235}\text{U}$  densities. It should be noted that each of the experimental points represents several different stackings of the  $\text{U}_3\text{O}_8$ -Sterotex blocks. As noted, the experimental data include some aluminum, and, as closely as possible, the proper amount was included in the calculation. The trend in Table X is qualitatively similar to that for the  $\text{UO}_2\text{F}_2$  experiments; the calculation seems to be relatively high for the lower  $H/^{235}\text{U}$  ratios and relatively low for the higher values of  $H/^{235}\text{U}$ .

These two sets of experiments were examined directly as was done for the  $\text{U}(30)\text{O}_2$ -wax experiments, but, if desired, the  $\text{UO}_2\text{F}_2$  data of Table IX may be converted to metal-water systems (as described earlier) and compared to the calculations given in Table VIIIa (or vice versa). The critical radii in Table IX may be converted to metal-water systems, but with some difficulty. A compositional correction scheme may be invented by identifying pairs of numbers -- metal-water and  $\text{U}_3\text{O}_8$ -Sterotex radii (Tables VIIIa and X) -- for the same  $H/^{235}\text{U}$ , but differing  $^{235}\text{U}$  density. A density correction on the sphere radius of the metal-water core to the density of the  $\text{U}_3\text{O}_8$ -Sterotex core will then define a new system with the extraneous atoms removed. An  $\bar{R}$  (Section IV) may then be defined.

#### D. Uranium Enriched to Three Percent, U(3)

Data are limited at this  $^{235}\text{U}$  enrichment and consist of a single critical assembly<sup>(48)</sup> and a series of measurements<sup>(49)</sup> of  $k_\infty$ , the infinite multiplication factor, at several moderations. The critical assembly was constructed of blocks of a  $\text{UF}_4$ -paraffin mixture in which the  $H/^{235}\text{U}$  ratio was 133.5 with a  $^{235}\text{U}$  density of  $9.33 \times 10^{-2} \text{ g/cm}^3$ . The experimental sphere radius (converted from a parallelepiped) is 36.28

TABLE X.  $\text{U}(4.89)_3\text{O}_8$ -STEROTEX MIXTURES

Bare and Water-Reflected

$H/^{235}\text{U}$	$\rho(^{235}\text{U})$ ( $\text{g/cm}^3$ )	Unreflected			Water-Reflected		
		Exp (cm)	Theory (cm)	Ratio	Exp (cm)	Theory (cm)	Ratio
6.37 +1	1.25 -1				38.038	-	
8.27 +1	1.07 -1				33.90	-	
1.24 +2	8.92 -2	37.48	39.409	1.052	29.97	31.374	1.047
1.47 +2	8.31 -2	35.77	36.809	1.029	29.21	29.448	1.008
2.45 +2	5.55 -2	34.05	35.304	1.037	27.18	28.519	1.049
3.20 +2	4.91 -2	32.44	32.055	0.988	26.42	26.369	0.998
3.95 +2	4.06 -2	33.21	33.129	0.998	26.67		
5.04 +2	3.33 -2	33.81	34.103	1.009	28.45	28.793	1.012
7.57 +2	2.21 -2	41.30	40.644	0.984	36.07	35.313	0.979

cm, and the calculated value is 37.910 cm. Thus, the ratio of calculated radius to experimental radius is a rather unsatisfactory 1.045.

The  $k_{\infty}$  experiments made use of  $UO_2-CH_2$  mixtures in which the enrichment was 3.04% and the  $H/U = H/(^{235}U + ^{238}U)$  atom ratio was varied from 3.58 to 47.98. Typical results are displayed in Table XI with calculational results at three moderations. Note that although the theory underestimates  $k_{\infty}$  at low moderations, it seems to be too high for the low density asymptote.

#### E. Uranium Enriched to Two Percent, U(2)

The one-dimensional critical parameters of U(2) metal-water systems and U(2) $O_2$ -water systems, bare and water-reflected, are given in Tables XIIa and XIIb, while the theoretical spherical radii are displayed in Fig. 12. The minimum critical volume is found at a  $^{235}U$  density of 0.066  $g/cm^3$  for the metal-water cores, but this minimum for the oxide core is at  $\sim 0.05$   $g/cm^3$ . The corresponding minima for the critical masses are  $\sim 0.047$  and  $\sim 0.037$   $g/cm^3$ .

The function relating  $^{235}U$  density and  $H/^{235}U$  moderation ratio in a metal-water

TABLE XI. INFINITE MULTIPLICATION FACTOR FOR 3% ENRICHED URANIUM

H/U	Experimental $k_{\infty}$	Theoretical $k_{\infty}$
3.58	1.310 $\pm$ 0.023	
5.86	1.346 $\pm$ 0.022	1.312
5.86	1.345 $\pm$ 0.020	
8.01	1.336 $\pm$ 0.020	
9.94	1.335 $\pm$ 0.018	
12.36	1.306 $\pm$ 0.016	
13.91	(1.298 $\pm$ 0.016)*	1.315
30.20	1.123 $\pm$ 0.008	
39.77	1.028 $\pm$ 0.007	
43.85	0.996 $\pm$ 0.006	1.055
47.98	0.955 $\pm$ 0.007	

\* Interpolated

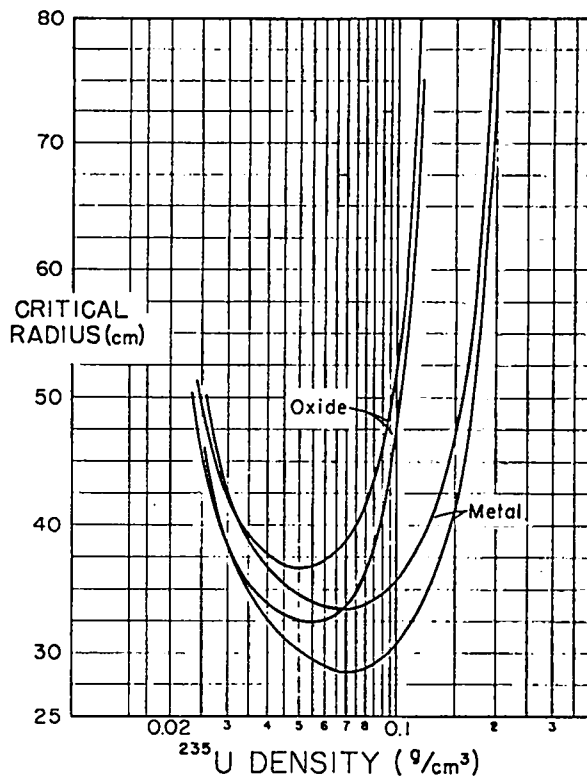


Fig. 12. Theoretical critical radii for U(2) metal-water and U(2) $O_2$ -water spheres, bare and water-reflected, vs  $^{235}U$  density. Comparison to experiment is given in Table XIII.

mixture is given by

$$\rho(^{235}U) = \frac{26.082}{68.475 + H/^{235}U} \quad (16)$$

The set of experimental critical data (50,51) for this enrichment is based solely on a series of experiments in which  $UF_4$  particles were mixed with paraffin. The  $^{235}U$  enrichment was 2.0 wt/%, and experiments were performed both bare and reflected with near-infinite paraffin. These data, along with a comparison to calculated results, are displayed in Table XIII. A possible trend noticed in some of the U(4.89) data and analyses seems to be duplicated here -- the theory predicts radii progressively higher as the moderation is decreased. Difficulties of this sort are not easy to resolve as the calculated radius is a most sensitive function of the as-

TABLE XIIa. U(2) METAL-WATER MIXTURES  
Critical Dimensions for Slabs, Cylinders, and Spheres

$H/^{235}\text{U}$	$^{235}\text{U}$ Density (g/cm <sup>3</sup> )	Unreflected			Water-Reflected		
		Slab Thickness (cm)	Cylinder Radius (cm)	Sphere Radius (cm)	Slab Thickness (cm)	Cylinder Radius (cm)	Sphere Radius (cm)
6.00 +1	2.03 -1	94.064	73.844	98.23	81.040	67.275	82.01
7.00 +1	1.88 -1	67.062	53.112	70.00	54.448	46.506	63.72
1.00 +2	1.55 -1	45.654	36.175	48.27	34.058	30.433	42.29
2.00 +2	9.72 -1	32.694	26.128	35.26	23.092	21.478	30.30
4.00 +2	5.57 -1	31.448	25.426	33.90	22.848	21.041	29.44
7.00 +2	3.40 -2	36.806	29.409	39.28	28.712	25.360	35.14
9.00 +2	2.70 -2	44.580	35.425	47.10	36.598	31.356	43.39

TABLE XIIb. U(2)O<sub>2</sub> METAL OXIDE-WATER MIXTURES  
Critical Dimensions for Slabs, Cylinders, and Spheres

$H/^{235}\text{U}$	$^{235}\text{U}$ Density (g/cm <sup>3</sup> )	Unreflected			Water-Reflected		
		Slab Thickness (cm)	Cylinder Radius (cm)	Sphere Radius (cm)	Slab Thickness (cm)	Cylinder Radius (cm)	Sphere Radius (cm)
7.00 +1	1.26 -1			134.91			
7.60 +1	1.23 -1						103.65
1.00 +2	1.10 -1			63.14			57.73
1.37 +2	9.55 -2						44.62
2.00 +2	7.75 -2			40.59			
2.30 +2	7.12 -2						33.99
4.00 +2	4.86 -2			36.57			
4.22 +2	4.78 -2						32.85
7.00 +2	3.12 -2			41.07			37.17
9.00 +2	2.52 -2			48.76			
9.64 +2	2.39 -2						48.79

TABLE XIII. U(2.0)F<sub>4</sub>-PARAFFIN MIXTURES  
Bare and Paraffin-Reflected

$H/^{235}\text{U}$	$\rho(^{235}\text{U})$ (g/cm <sup>3</sup> )	Unreflected			Paraffin-Reflected		
		Exp (cm)	Radius Theory (cm)	Ratio	Exp (cm)	Radius Theory (cm)	Ratio
1.96 +2	6.28 -2	44.93	47.32	1.053	39.43	41.11	1.043
2.93 +2	5.31 -2	38.39	40.25	1.048	33.59	34.97	1.041
4.04 +2	4.45 -2	36.46	38.05	1.044	32.26	33.34	1.034
5.01 +2	3.94 -2	36.40	37.22	1.023	32.00	32.93	1.029

sumed  $^{238}\text{U}$  cross sections and these are not especially well-known. A value of  $k$  was calculated using the experimental radius for the bare core of  $\text{H}/^{235}\text{U} = 195.6$  and  $\rho(25) = 0.0628$  in Table XIII. This turned out to be 0.986, an error of only 1.4%, whereas the critical radius is missed by 5.3%. Additional experiments would be most useful.

To my knowledge, no  $\text{UO}_2\text{F}_2$  solution experiments have been performed at this enrichment. Since the solution density limit is about 1.0 g total uranium/cm<sup>3</sup>, the upper limit for  $^{235}\text{U}$  density would be only 0.02 g/cm<sup>3</sup>, a density possibly inadequate for a critical system. At this enrichment, the metal-water standard, as always, gives minimal values, but these may be nearly impossible of attainment.

Two careful  $k_{\infty}$  experiments (52) have been completed with  $\text{U}(2)\text{F}_4$ -paraffin compacts at an  $\text{H}/^{235}\text{U}$  moderation ratio of 195. The theoretical value of  $k_{\infty} = 1.157$  is ~4% lower than the experimental measurements of  $1.216 \pm 0.013$  and  $1.197 \pm 0.015$ .

#### F. Uranium Enriched to 1.42 Percent, $\text{U}(1.42)$

The experimental data (43) pertinent to uranium enriched to 1.42% (the lowest enrichment known to have been used in a homogeneous critical assembly) are presented in Table XIV. The fuel for these experiments was a mixture of  $\text{UF}_4$  and paraffin manufactured into unclad blocks of several different sizes and of two moderations,  $\text{H}/^{235}\text{U} = 418$  and  $\text{H}/^{235}\text{U} = 562$ . The remaining experiments of differing  $\text{H}/^{235}\text{U}$  ratios were with heterogeneous structures constructed by mixing blocks of paraffin with the fuel. The basic experiments were performed with a polyethylene reflector, and results for the water-reflected or unreflected cases were obtained by study of the reflector saving on one face. (Data for some other reflectors are given in Section VII.) Most of the experiments were in the form of parallelepipeds, but some few were pseudo-cylinders; all of these experimental dimensions have been converted to spheres using  $\delta' = 8$  cm (defined in Section II), a value giving the most nearly invariant radius for the eight differently shaped critical assemblies using the  $\text{H}/^{235}\text{U} = 418$  fuel.

TABLE XIV.  $\text{U}(1.42)\text{F}_4$ -PARAFFIN MIXTURES  
Bare, Paraffin, and Water-Reflected

$\text{H}/^{235}\text{U}$	$\rho(^{235}\text{U})$ (g/cm <sup>3</sup> )	Reflector	Core Character	Experimental Radius (cm)	Theoretical Radius (cm)	$\frac{R_{\text{DTK}}}{R_{\text{Exp}}}$
4.18 +2	3.53 -2	None	Homogeneous	58.70	65.06	1.11
5.62 +2	3.05 -2	"	"	59.30	66.38	1.12
4.18 +2	3.53 -2	Water	"	55.00	59.09	1.07
5.62 +2	3.05 -2	"	"	55.80	63.08	1.13
4.18 +2	3.53 -2	Polyethylene	"	54.15	58.86	1.09
4.56 +2	3.35 -2	"	Heterogeneous	53.78	-	-
4.65 +2	3.33 -2	"	"	53.60	-	-
4.94 +2	3.21 -2	"	"	53.78	-	-
5.31 +2	3.11 -2	"	"	53.89	-	-
5.62 +2	3.15 -2	"	Homogeneous	55.53	-	-
5.86 +2	2.94 -2	"	Heterogeneous	54.64	-	-
6.34 +2	2.81 -2	"	"	56.55	-	-
6.80 +2	2.64 -2	"	"	58.80	-	-



For these mixtures of UF<sub>4</sub> and polyethylene, the minimum critical volume is found at H/<sup>235</sup>U = 480 and ρ(<sup>235</sup>U) = 0.0334 g/cm<sup>3</sup>, and the minimum critical mass is located at H/<sup>235</sup>U = 530 and ρ(<sup>235</sup>U) = 0.031 g/cm<sup>3</sup>. Calculations of these low <sup>235</sup>U-content systems are disappointing. The theoretical radius seems to be 11 to 12% high for the bare cores, about 8% high for two of the reflected systems, and 13% high for the water-reflected point for which H/<sup>235</sup>U = 562. Again, the theory is extraordinarily sensitive to assumed <sup>238</sup>U cross sections. Despite these unsatisfactory results, the theoretical metal-water data are presented in Table XV. Although not shown, the minimum critical volume is found at H/<sup>235</sup>U = 400 and ρ(<sup>235</sup>U) = 0.055 g/cm<sup>3</sup>, and minimum critical mass at H/<sup>235</sup>U = 470 and ρ(<sup>235</sup>U) = 0.046 g/cm<sup>3</sup>. Clearly, if these data are to be used where high precision is required, caution is advisable. The relationship between <sup>235</sup>U metal density and the H/<sup>235</sup>U atom ratio is given by

$$\rho(^{235}\text{U}) = \frac{26.082}{96.436 + \text{H}/^{235}\text{U}} \quad (17)$$

#### G. Uranium Enriched to 1.03 Percent, U(1.03)

Of considerable interest to some operations with slightly enriched uranium is that minimum enrichment for which k<sub>∞</sub> is 1.0. Experiments<sup>(49)</sup> in the Physical Con-

stants Testing Reactor using fuel samples of several very low enrichments suggest that this minimum value is 1.03 ± 0.01 wt/% <sup>235</sup>U at an H/U atom ratio of about 4.7. The k<sub>∞</sub> is relatively insensitive to the moderation, and little difference exists between k<sub>∞</sub> values at, say, H/U ~ 4.3 and ~ 5.2. Some of these results have been examined by Roach.<sup>(13)</sup>

#### H. <sup>233</sup>U Systems

The critical radii, both theoretical and experimental,<sup>(53-56)</sup> for <sup>233</sup>U spheres are displayed in Figs. 13 and 14. Composition is the metal-water mixture for pure <sup>233</sup>U, and, in accord with the standard defined above, all containers are imagined to have been removed. Aside from one solid metal point<sup>(3)</sup> (not illustrated -- see Tables I and II), the experimental data were obtained by use of two different uranium salts in water, UO<sub>2</sub>F<sub>2</sub> and UO<sub>2</sub>(NO<sub>3</sub>)<sub>2</sub>. The corrections for conversion of UO<sub>2</sub>F<sub>2</sub> solutions to a metal-water system are taken to be the same as for <sup>235</sup>U, while  $\bar{R}$  for the nitrate salt (reflected systems) may be computed by substituting a = 1.957 in Eq. 11. In lieu of experiments or pertinent calculations, density exponents were taken to be equal to those for plutonium systems. A special correction to many of these <sup>233</sup>U data was to change the reflector from paraffin to water -- paraffin being the better

TABLE XV. U(1.42) METAL-WATER MIXTURES  
Critical Dimensions for Slabs, Cylinders, and Spheres

H/ <sup>235</sup> U	<sup>235</sup> U Density (g/cm <sup>3</sup> )	Unreflected			Water-Reflected		
		Slab Thickness (cm)	Cylinder Radius (cm)	Sphere Radius (cm)	Slab Thickness (cm)	Cylinder Radius (cm)	Sphere Radius (cm)
1.70 +2	9.79 -2			70.46			63.84
2.00 +2	8.80 -2	57.96	45.93	60.87	47.58	40.48	55.40
3.50 +2	5.84 -2	46.81	37.18	49.33	37.48	32.32	44.57
5.00 +2	4.37 -2	48.69	38.59	51.19	39.91	34.08	46.78
7.50 +2	3.08 -2	62.08		64.98	54.07	44.70	60.37
9.00 +2	2.62 -2			84.92			
1.00 +3	2.38 -2				103.80	83.71	113.78

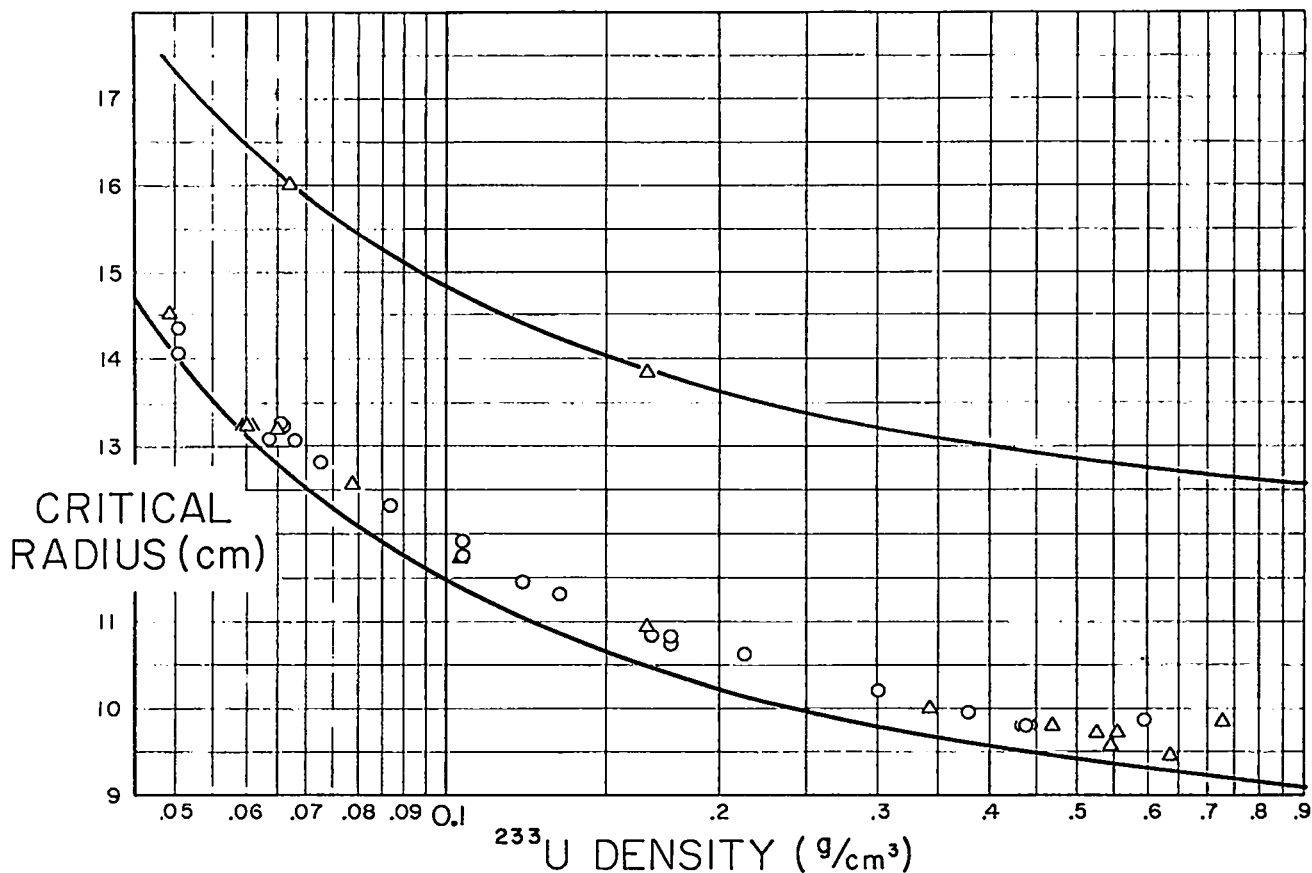


Fig. 13. Critical radii for  $^{233}\text{U}$  metal-water spheres, bare and water-reflected, vs  $^{233}\text{U}$  density. The experimental data are described in References 53 - 56 while the solid line is theoretical. Unreflected experiments are few, and the theory is disappointingly low for the water-reflected cores.

of the two. This function was defined by four special problems, and to change the reflector from paraffin to water, the critical radius must be increased by 0.14, 0.27, 0.275, and 0.18 cm at  $\text{H}/^{235}\text{U}$  ratios of 0.0, 30.0, 57.5, and 300. Container corrections -- mostly for aluminum -- were assumed to be equal to those for  $^{235}\text{U}$  systems. Theoretical values for the critical parameters of a wide range of metal-water mixtures, bare and water-reflected, are given in Table XVI.

The data, as corrected and illustrated in Figs. 13 and 14, suggest that the theory predicts radii low by at least 3% for the higher  $^{233}\text{U}$  solution densities (Fig. 13) and low by about 2% for the more dilute cores (Fig. 14). The calculation matches the few unreflected solution experiments

quite well, and the metal data of Tables I and II are reproduced accurately. However, as for  $\text{U}(93.5)$ , precision for the metal systems is not entirely accidental. Data obtained from the two paraffin-reflected solutions,  $\text{UO}_2\text{F}_2$  and  $\text{UO}_2(\text{NO}_3)_2$ , are consistent with each other and with the few water-reflected experiments. The low  $^{233}\text{U}$  density asymptote ( $k_\infty = 1.0$ ) is found by calculation to be at an  $\text{H}/^{233}\text{U}$  atom ratio of 2314.

The relationship between  $^{233}\text{U}$  densities and  $\text{H}/^{233}\text{U}$  atom ratios in metal-water mixtures is given by

$$\rho(^{233}\text{U}) = \frac{25.86}{1.405 + \text{H}/^{233}\text{U}} \quad (18)$$

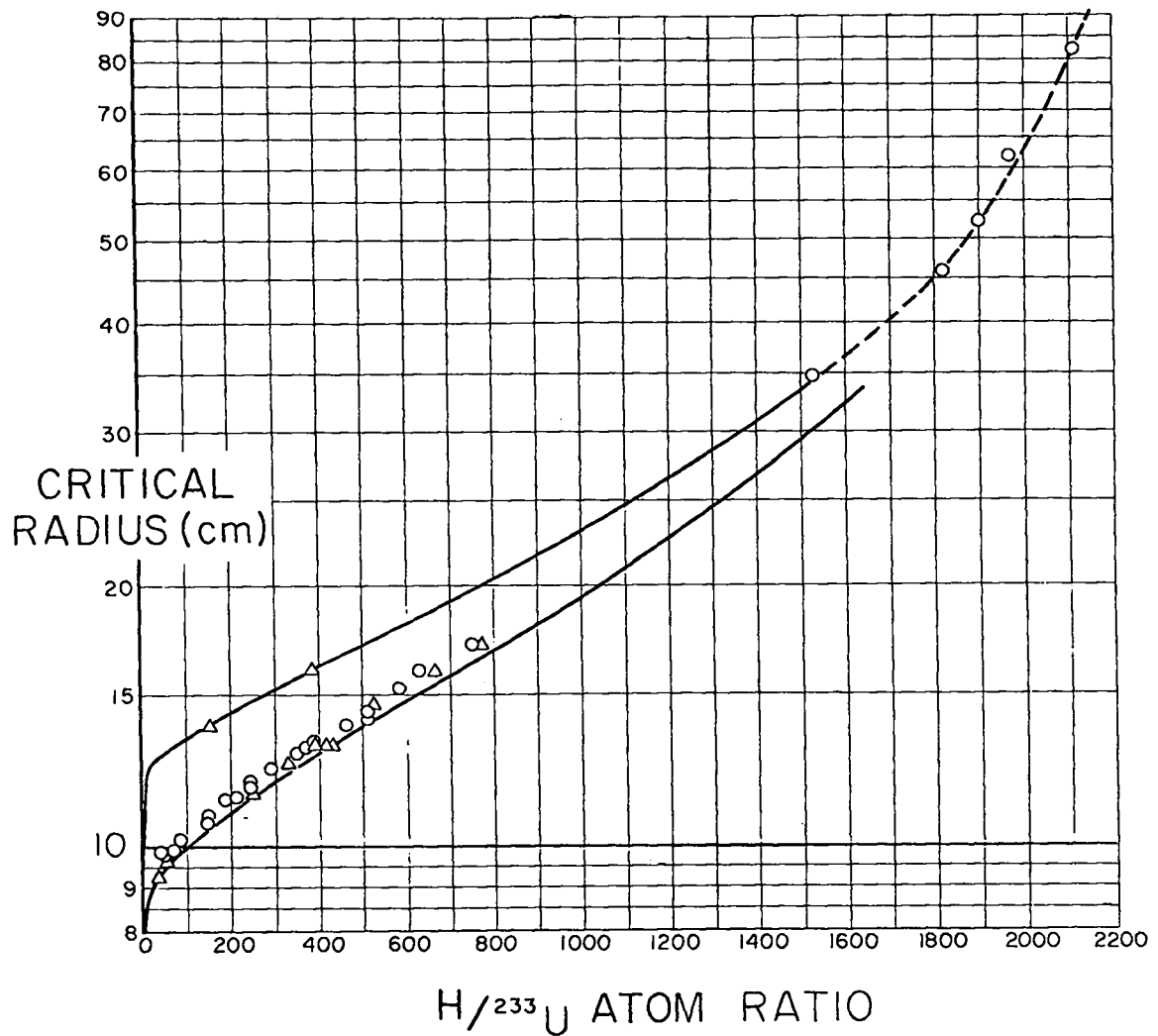


Fig. 14. Critical radii for <sup>233</sup>U metal-water spheres, bare and water-reflected, vs the H/<sup>233</sup>U atom ratio.

TABLE XVI. <sup>233</sup>U METAL-WATER MIXTURES

Critical Dimensions for Slabs, Cylinders, and Spheres

H/ <sup>233</sup> U	<sup>233</sup> U Density (g/cm <sup>3</sup> )	Unreflected			Water-Reflected		
		Slab Thickness (cm)	Cylinder Radius (cm)	Sphere Radius (cm)	Slab Thickness (cm)	Cylinder Radius (cm)	Sphere Radius (cm)
0.0	1.87 +1	4.204	3.954	5.743	0.737	2.449	4.500
1.00 +0	1.08 +1	5.994	5.433	7.745	1.132	3.260	5.841
3.00 +0	5.90 +0	7.978	7.010	9.858	1.647	4.150	7.246
1.00 +1	2.27 +0	9.906	8.519	11.853	2.400	5.047	8.546
3.00 +1	8.24 -1	10.708	9.107	12.608	3.062	5.500	9.125
1.00 +2	2.55 -1	11.544	9.716	13.379	4.176	6.179	9.934
3.00 +2	8.58 -2	13.426	11.138	15.252	6.398	7.724	11.882
5.00 +2	5.16 -2	15.324	12.599	17.145	8.428	9.236	13.837
1.00 +3	2.58 -2	21.128	17.049	23.009	14.300	13.725	19.480
1.50 +3	1.72 -2	30.798	24.379	33.238	23.686	21.021	29.254

## I. Plutonium Systems

Theoretical values for the one-dimensional parameters of plutonium metal-water systems are presented in Table XVII and illustrated, in part, in Figs. 15 and 16. These data have been calculated for 100%  $^{239}\text{Pu}$ ,  $\text{Pu}(100)$ , and the effects of dilution of  $^{240}\text{Pu}$  by varying amounts may be estimated by application of the theoretical data<sup>(13)</sup> given in Fig. 17 which shows the dependence of the plutonium critical mass upon the  $^{240}\text{Pu}$  content, displayed as a function of the  $\text{H}/^{239}\text{Pu}$  atom ratio. As in the case of uranium, the metal-water mixture is a useful standard because of its maximum density (minimum mass) and, especially here, the nonambiguity of the solution components.

The experimental critical data for plutonium systems have been obtained with four general types of core materials:  $\text{PuO}_2(\text{NO}_3)_2$ -water solutions,<sup>(57-60)</sup>  $\text{PuO}_2$ -hydrocarbon compacts,<sup>(27,42)</sup> metal,<sup>(3)</sup> and interleaved metal and plastic plates.<sup>(61-63)</sup> Many of the known results of experiment are displayed in Fig. 15 or Fig. 16.

Conversion of plutonyl nitrate solution dimensions to metal-water mixtures is often difficult because of the frequent ex-

perimental necessity of adding excess nitric acid (the amount of which may not be known precisely) to the solution to ensure continued solubility of the salt. Introducing nitric acid increases the critical mass -- water is displaced, changing the  $\text{H}/\text{Pu}$  ratio, and nitrogen has higher parasitic absorption than the displaced hydrogen. The magnitude of the change is not obvious, however. For a limited range of plutonium densities,  $\text{H}/\text{Pu}$  ratios, and nitrate ion concentrations, the experimental data<sup>(57)</sup> of Fig. 18 can be used to estimate the influence of excess nitric acid upon the critical mass; note, however, that undermoderated solutions are not included. Recent and confirming results<sup>(58)</sup> (not illustrated) in the general range of Fig. 18 are available and allow better extrapolations to the zero nitrate mixture. As in the case of uranium solutions, a theoretical correction function for the poisoning effect of a stainless steel container placed between the core and water reflector was generated, this function being close to that for uranium (Fig. 6) at the same moderation ratio. Greater precision may be obtained if the  $\Delta R$  read from the curve on Fig. 6 is reduced by  $\sim 0.07$  cm at  $\text{H}/\text{Pu}$  ratios of 200 and 500.

TABLE XVII.  $^{239}\text{Pu}$  METAL-WATER MIXTURES  
Critical Dimensions for Slabs, Cylinders, and Spheres

$\text{H}/^{239}\text{Pu}$	$^{239}\text{Pu}$ Density ( $\text{g}/\text{cm}^3$ )	Unreflected			Water-Reflected		
		Slab Thickness (cm)	Cylinder Radius (cm)	Sphere Radius (cm)	Slab Thickness (cm)	Cylinder Radius (cm)	Sphere Radius (cm)
0.0	1.97 +1	3.518	3.421	4.900	0.817	2.266	3.983
1.00 +0	1.13 +1	5.540	5.000	7.148	1.322	3.117	5.481
3.00 +0	6.11 +0	7.598	6.669	9.382	2.034	4.123	7.037
1.00 +1	2.34 +0	10.242	8.766	12.166	3.276	5.497	9.060
3.00 +1	8.46 -1	12.066	10.187	14.050	4.354	6.508	10.495
1.00 +2	2.62 -1	13.088	10.996	15.101	5.260	7.219	11.415
3.00 +2	8.81 -2	14.082	11.742	16.069	6.596	8.099	12.494
5.00 +2	5.29 -2	15.034	12.463	17.006	7.770	8.917	13.520
1.00 +3	2.65 -2	17.804	14.588	19.792	10.810	11.168	16.423
2.00 +3	1.33 -2	25.942	20.883	28.057	19.140	17.535	24.733

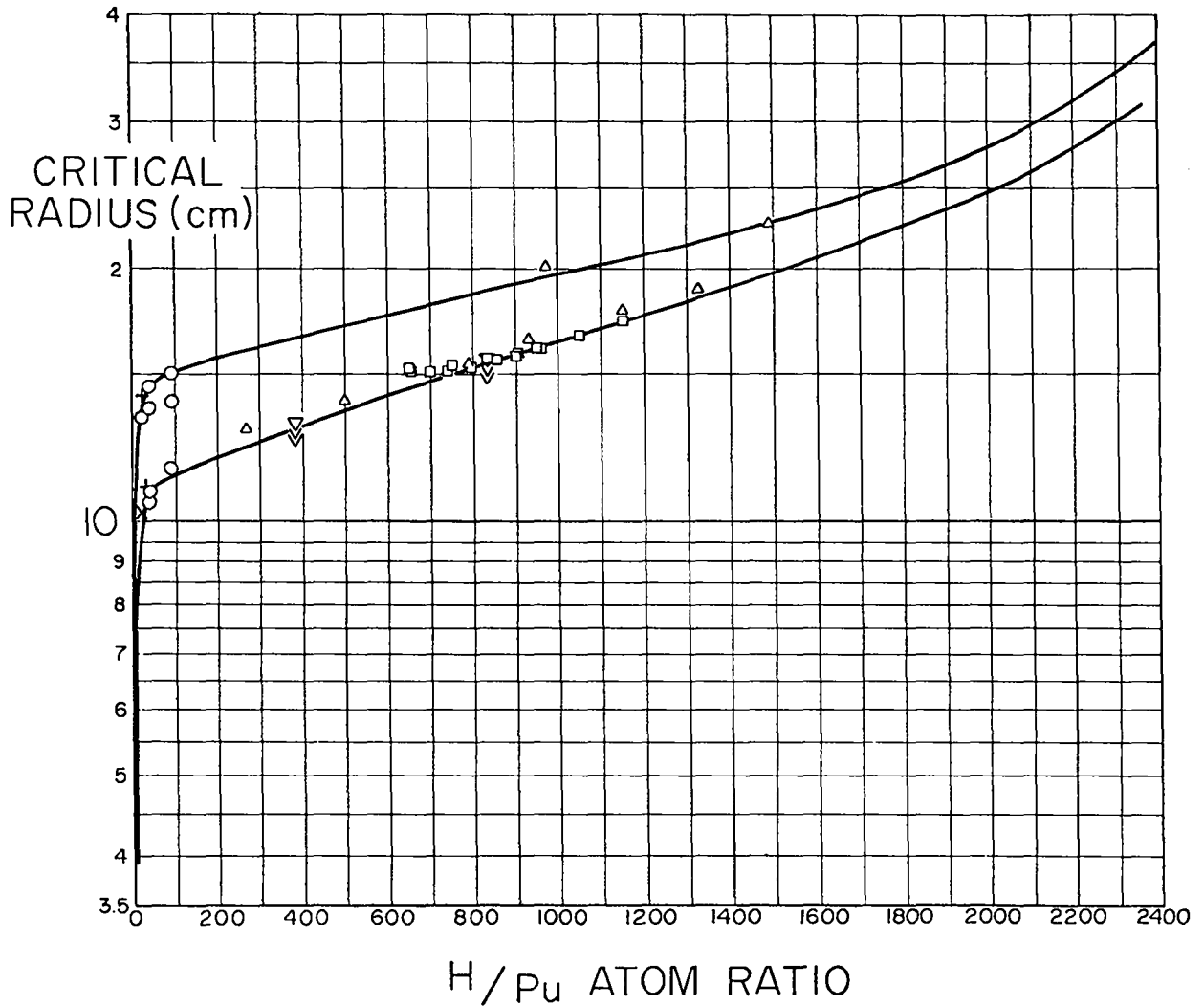


Fig. 15. Critical radii for  $^{239}\text{Pu}$  metal-water spheres, bare and water-reflected, vs the  $\text{H}/^{239}\text{Pu}$  atom ratio. Symbols and references for this figure and for Fig. 16 are:  $\Delta$ , 57;  $\nabla$ , 58;  $\square$ , 59, 60;  $\times$ , 43;  $+$ , 27. The solid line is theoretical.

The  $\text{PuO}_2(\text{NO}_3)_2$ -water data reduced to a metal-water, no container basis are displayed in Fig. 15 along with the theoretical values and some few metal plate-lucite data (also on a metal-water basis). In general, the internal consistency of the experimental data obtained from different laboratories is satisfactory, and the theory reproduces the experiments reasonably well. This comforting situation is contradicted at extreme dilutions by the calculated and experimental values for the  $^{239}\text{Pu}$

density required to maintain  $k_\infty$  at unity. These are  $7.0$  and  $8.0 \pm 0.3 \times 10^{-3}$  (64)  $\text{g}/\text{cm}^3$ , respectively; the discrepancy is not understood.

The data obtained from  $\text{PuO}_2$ -polystyrene and  $\text{PuO}_2$ -polyethylene compacts and from plutonium metal plates interleaved with lucite plates are shown in Fig. 16 as a function of the  $\text{H}/^{239}\text{Pu}$  ratio. In this case the data are illustrated relative to a metal-lucite mixture, even though each experiment was calculated directly with its

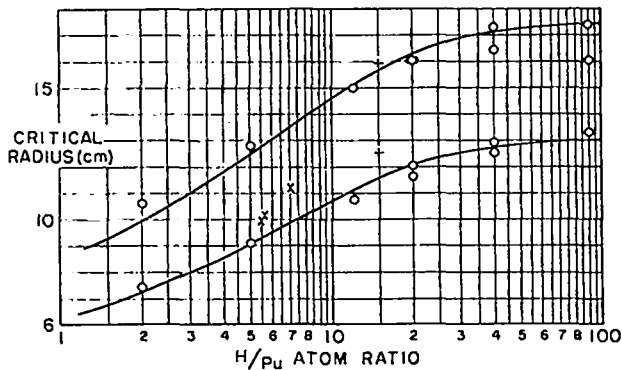


Fig. 16. Critical radii vs  $H/^{239}\text{Pu}$  atom ratio for bare and lucite-reflected cores of plutonium metal-lucite mixtures. Experiments employing different materials were adjusted to this mixture. Symbols are defined in the caption for Fig. 15. The solid line is theoretical.

own materials. Where possible, the reflector saving used for shape conversion was taken from the experiments, otherwise, a

value was calculated. At best, one must conclude that some doubt exists as to the true values of the critical parameters in this general range of  $H/\text{Pu}$  and plutonium densities.

It should be noted that sundry difficulties attended the experiments with  $\text{PuO}_2$ -polyethylene compacts and plutonium metal-lucite plates. The former were not stable chemically -- the alpha-particle activity continuously generated hydrogen gas, thus placing the  $H/\text{Pu}$  ratio in doubt and the ratio also suffered from heterogeneity effects and a requirement that experiments be quite subcritical. To correct the metal-lucite experimental results to homogeneous systems, a special set of experiments was performed with successively thinner plates. Experimental errors were estimated to be as much as 5 or 6% on the radius, but the data seem to show internal consistency somewhat

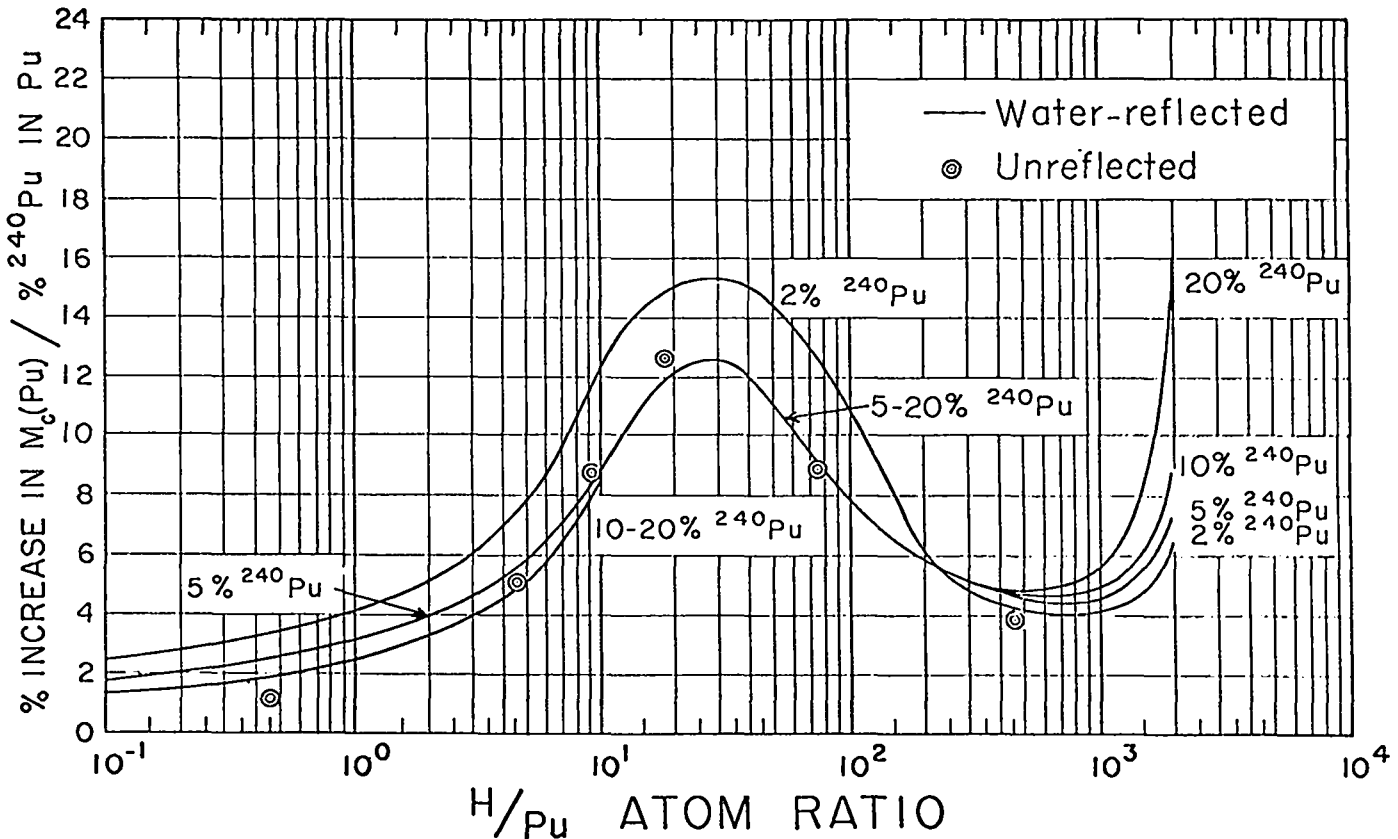


Fig. 17. Computed influence of  $^{240}\text{Pu}$  on the critical mass of metal-water spheres. The solid lines are from Roach<sup>(13)</sup> and represent reflected spheres. The points are for bare systems and were calculated by G. I. Bell and C. B. Mills<sup>(14)</sup> with an 18-group cross section set and the DSN transport code.

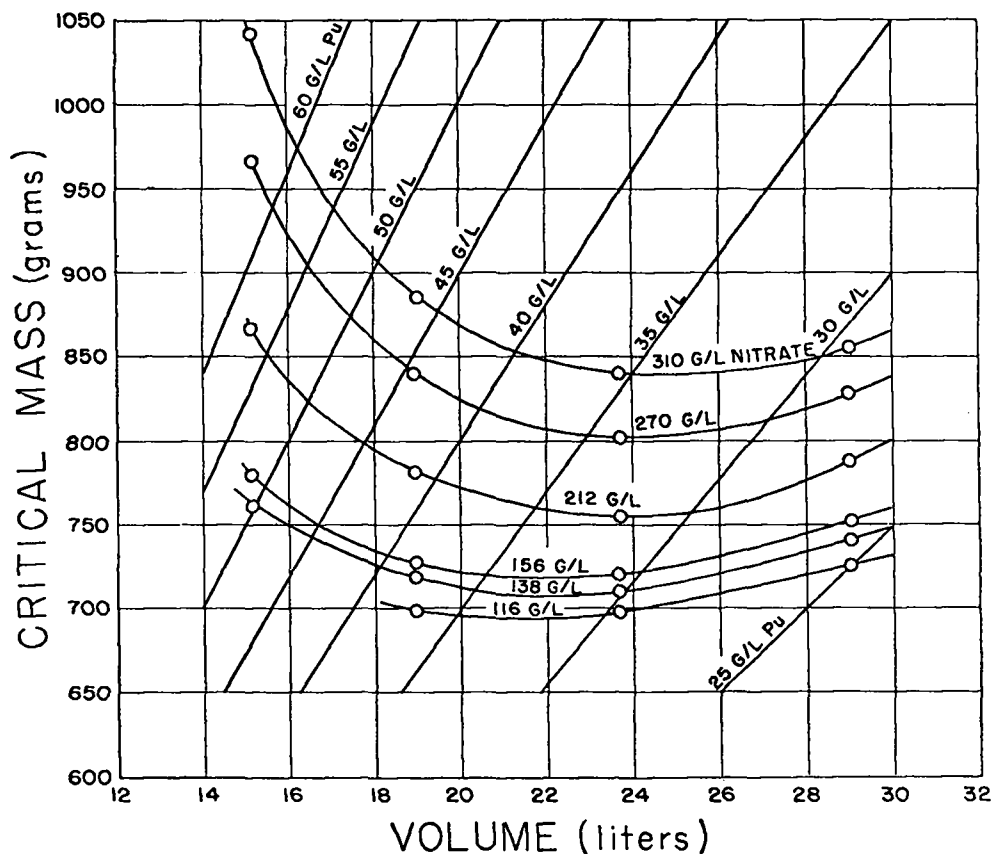


Fig. 18. Critical mass of water-reflected  $\text{PuO}_2(\text{NO}_3)_2$  spheres vs volume for varying amounts of excess  $\text{HNO}_3$ . The  $^{240}\text{Pu}$  content was 3.12%, and the spheres include a 1/16-in.-stainless steel sphere.

better than this. These metal-lucite points shown on Fig. 16 were taken from smoothed plots of the more numerous experimental, cylindrical data; hence the precise values of H/Pu. At the time of writing, the  $\text{PuO}_2$ -polystyrene experimental results are preliminary but are not expected to be changed significantly. These last experiments are several in number, all at the same H/Pu = 15.0.

The relationship between  $^{239}\text{Pu}$  density and H/Pu moderation ratio in metal-water mixtures is given by

$$\rho(^{239}\text{Pu}) = \frac{26.527}{1.353 + \text{H}/^{239}\text{Pu}} \quad (19)$$

#### VI. INTERNAL MODERATION (DEUTERIUM, BERYLLIUM AND OXYGEN)

Some limited experimental data are

available for cores of U(93.5) moderated by  $\text{D}_2\text{O}$ ,<sup>(65)</sup> Be,<sup>(66)</sup> and BeO.<sup>(67)</sup> These data are shown in Fig. 19, for which the critical volume is chosen as the ordinate to illustrate the tremendous variation of this parameter as a function of fissile atom density. The data in Reference 68 are also of interest here. For comparison of form, the pertinent U(93.5)-water and U(93.5)-graphite critical volumes from Table V are included. Experimental points with the Be, BeO, and  $\text{D}_2\text{O}$  moderators are indicated on each curve, and the solid line represents the results of theory, in this case DSN, 18-group calculations by C. B. Mills.<sup>(69)</sup>

To my knowledge, comparable data for plutonium,  $^{233}\text{U}$ , and other  $^{235}\text{U}$  enrichments do not exist.

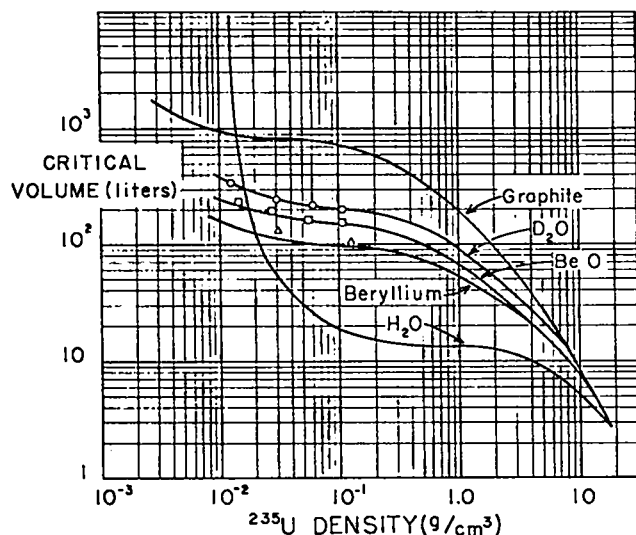


Fig. 19. Bare critical volume vs  $^{235}\text{U}$  density for several U(93.5) metal moderator mixtures. The data for water and graphite are taken from Table V while those for Be, BeO, and  $\text{D}_2\text{O}$  are due to C. B. Mills. (69) For all metal-moderator mixtures, the critical volume increases monotonically with decreasing  $^{235}\text{U}$  density.

## VII. REFLECTORS

### A. Thickness, Gaps, and Density

The basic function of a reflector is to return neutrons to the core where they can cause fissions and thus reduce the amount of fissile material required to maintain the critical state. Some gamma and neutron shielding is also obtained, a sometimes useful property but of no interest here. The degree to which a given material performs the reflection function depends on the neutron spectrum, reflector thickness, density, purity, and (with the exception of very large planes or slabs) distance from the core. Some of these characteristics for a few materials of interest will be examined; both experimental and theoretical data are available.

In general it may be noted that all materials, even strong poisons such as boron or cadmium, can be effective reflectors, as the only requirement is that the

TABLE XVIII. (3, 18) CRITICAL MASSES OF U(93.5) METAL, VARIOUS REFLECTORS

Reflector	Density (g/cm <sup>3</sup> )	Critical Mass, kg $^{235}\text{U}$ in sphere, $\rho(^{235}\text{U}) = 17.6 \text{ g/cm}^3$ Data Adjusted to the Following Reflector Thicknesses				
		0.5 in.	1 in.	2 in.	4 in.	infinite
Beryllium	1.84	35.1	28.1	20.8	14.1	~ 7.0
BeO	2.69	—	—	21.3	15.5	~ 8.9
Graphite(CS-312)	1.67	39.3	34.4	29.5	24.2	14.5
Paraffin	—	—	—	—	—	21.8
Polyethylene	—	38.9	30.8	—	—	—
Water	—	—	—	~ 24.0	22.9	22.8
Heavy Water	—	—	—	~ 27.0	21.0	~ 11.5
Magnesium	1.77	42.5	39.9	—	—	—
Aluminum	2.70	41.7	38.1	~ 35.5	~ 32.0	< 30.0
$\text{Al}_2\text{O}_3$	2.76	38.9	34.1	—	—	—
Titanium	4.50	41.9	38.6	—	—	—
Iron	7.87	38.5	34.1	29.3	25.3	23.2
Cobalt	8.72	36.7	31.2	—	—	—
Nickel	8.88	36.4	31.2	25.7	~ 21.5	19.6
Copper	8.88	37.1	31.3	25.4	20.7	—
Zinc	7.04	—	—	29.8	25.0	—
Molybdenum	10.53	36.9	31.0	—	—	—
Lead	11.30	—	—	—	29.5	—
Thorium	11.48	—	—	33.3	—	—
Uranium	19.0	35.6	29.3	23.5	18.4	16.1



scattering cross section be finite. All materials exhibit the property of "saturation"; that is, increasing the thickness indefinitely beyond some value does not result in any additional saving of core fissile material. Incorporation of a poison in a reflector results only in a lessening of the saturation thickness. The most effective reflector poison is an unlimited void, as only such a volume absorbs all neutrons entering it. As we have noted, the effect of a reflector is expressed in terms of a reflector saving. This reflector saving is often and conveniently expressed as a distance -- the change of critical radius when the reflector is added (see Section III).

Experimental data<sup>(3,18)</sup> for a wide variety of reflectors of differing thicknesses surrounding spherical U(93.5) metal cores are presented numerically in Table XVIII. The saturation property is quite evident for the water, iron, and uranium reflectors, while the moderating but nearly noncapturing materials such as beryllium, graphite, and D<sub>2</sub>O require much greater thicknesses before exhibiting this property.

Some of these experiments have been examined theoretically; as mentioned earlier, those with uranium reflection were basic to the development of the cross-section set. The data for reflection by normal uranium are predicted to within 1.5% (theory low) on radius by S<sub>4</sub>, and almost exactly by the S<sub>8</sub> approximation. The graphite-reflected calculations are low by ~1.6% for reflector thicknesses between 2 and 12 cm, are exact at 20 cm, and high by ~1% for thicknesses greater than 30 cm. The water-reflected point at 10.16 cm is calculated ~1.4% high in the S<sub>4</sub> approximation.

To extend the experimental data of Table XVIII, some additional theoretical parametric studies have been completed. The first of these is the set of critical data for spheres of U(93.5)-graphite mixtures reflected by various thicknesses of

graphite (pure, constant density at 1.90 g/cm<sup>3</sup>). The core mixtures have C/<sup>235</sup>U ratios of 0.0, 17.77, 77.48, and 2545.0 (identical to some presented in Table V), and reflector thicknesses extend to 200 cm to ensure saturation. These data are given in detail in Table XIX and illustrated in part in Fig. 20. Clearly, the C/<sup>235</sup>U ratio influences the thickness required for saturation; about 60 cm is needed for the metal core, but ~200 cm for the core of C/<sup>235</sup>U = 2545. The reflector saving may be obtained from the table.

Another set of computations is presented in Table XX in which spherical cores of three different metal-water mixtures (H/<sup>235</sup>U = 0.0, 30.0, and 300) are surrounded by various thicknesses of lucite, polyethylene, water, graphite, and liquid hydrogen ( $\rho = 0.07 \text{ g/cm}^3$ ). Water reflection data from this table are illustrated in Fig. 21 in which the ratio of reflected to bare critical mass is plotted as a function of the water thickness. It is of interest to note that the hydrocarbon reflectors saturate at about 10 cm thickness, very much less than that required by graphite, for example. This saturation property may be ascribed to the action of hydrogen as a mild poison following its moderation of the neutrons; those neutrons thermalized far into the reflector are captured before a return to the core is achieved. The data for liquid hydrogen and graphite suggest that the heavier atom concentration in the reflector is indeed important.

Some experimental reflector thickness results are available for U(30)O<sub>2</sub>-paraffin mixtures,<sup>(24)</sup> a part of the same experiments discussed in Section Vb. In these experiments the <sup>235</sup>U density was 0.331 g/cm<sup>3</sup> with H/<sup>235</sup>U = 81.8; the core was a parallelepiped with a base 7 x 7 in., reflected on five sides with 8 in. of polyethylene, while the sixth side had a variable thickness of the same material. The information is given most easily in terms of the reflector sav-

TABLE XIX. CRITICAL RADII OF FOUR U(93.5) METAL-GRAPHITE CORES, GRAPHITE-REFLECTED

$C/^{235}\text{U}$	$^{235}\text{U}$ Density ( $\text{g}/\text{cm}^3$ )	Reflector Thickness (cm)	Critical Radius (cm)	Critical Mass (cm)	M(reflected) M(bare)
0.0	1.76 +1	0.0	8.649	47.70	1.000
0.0	1.76 +1	1.0	8.125	39.55	0.829
0.0	1.76 +1	4.0	7.247	28.05	0.588
0.0	1.76 +1	12.0	6.366	19.03	0.399
0.0	1.76 +1	30.0	5.782	14.25	0.299
0.0	1.76 +1	100.0	5.459	11.99	0.251
0.0	1.76 +1	200.0	5.437	11.85	0.248
1.777 +1	1.87 +0	0.0	29.167	194.46	1.000
1.777 +1	1.87 +0	1.0	28.268	177.03	0.910
1.777 +1	1.87 +0	4.0	25.879	135.83	0.698
1.777 +1	1.87 +0	12.0	21.460	77.46	0.398
1.777 +1	1.87 +0	30.0	16.831	37.37	0.192
1.777 +1	1.87 +0	100.0	14.049	21.73	0.112
1.777 +1	1.87 +0	200.0	13.835	20.75	0.107
7.748 +1	4.67 -1	0.0	44.784	175.89	1.000
7.748 +1	4.67 -1	1.0	43.867	165.31	0.940
7.748 +1	4.67 -1	4.0	41.122	136.17	0.774
7.748 +1	4.67 -1	12.0	34.868	83.02	0.472
7.748 +1	4.67 -1	30.0	25.789	33.59	0.191
7.748 +1	4.67 -1	100.0	19.825	15.26	0.087
7.748 +1	4.67 -1	200.0	(19.5)		
2.545 +3	1.46 -2	0.0	59.980	13.21	1.000
2.545 +3	1.46 -2	1.0	59.069	12.61	0.967
2.545 +3	1.46 -2	4.0	56.137	10.83	0.831
2.545 +3	1.46 -2	12.0	48.795	7.11	0.545
2.545 +3	1.46 -2	30.0	37.494	3.226	0.247
2.545 +3	1.46 -2	100.0	29.771	1.615	0.124
2.545 +3	1.46 -2	200.0	29.364	1.550	0.119

ing for the one face for given thicknesses of polyethylene:

Reflector Thickness:	1 in.	2 in.	4 in.	6 in.	8 in.
ΔR	: 0.76 in.	1.11 in.	1.32 in.	1.34 in.	1.38 in.

There has been no attempt to calculate these quantities.

Similar data have been obtained with the  $\text{U}(1.42)\text{F}_4$ -paraffin assembly<sup>(43)</sup> discussed in Section Vf. In this case the assembly base size was either 45 x 45 in. or 48 x 48 in., and the assembly rested on a bed of polyethylene 8-in. thick. To determine the reflector saving, the critical height was measured with and without top layers of the reflector material under scrutiny. The reflector saving was thus determined for a number of materials of various thicknesses both without and with a 0.030-in.-thick layer of cadmium placed between

the core and reflector. For thick reflectors this poison invariably reduced the reflector saving (increased the critical mass), but for thin reflectors the influence of cadmium is less clear, and for one case, the cadmium actually increased the reflector saving. The reported value of the reflector saving of cadmium by itself was 0.6 cm.

These results are given in Table XXI and illustrated in Fig. 22. The graphite, concrete, and mild steel densities were 1.65, 2.3, and 7.8  $\text{g}/\text{cm}^3$ , respectively. The steel is described as B. S. 15 No. 1 quality, while the concrete is not further described. All the materials considered here show the saturation property, except for graphite, for which, as noted above, extreme thicknesses are required.

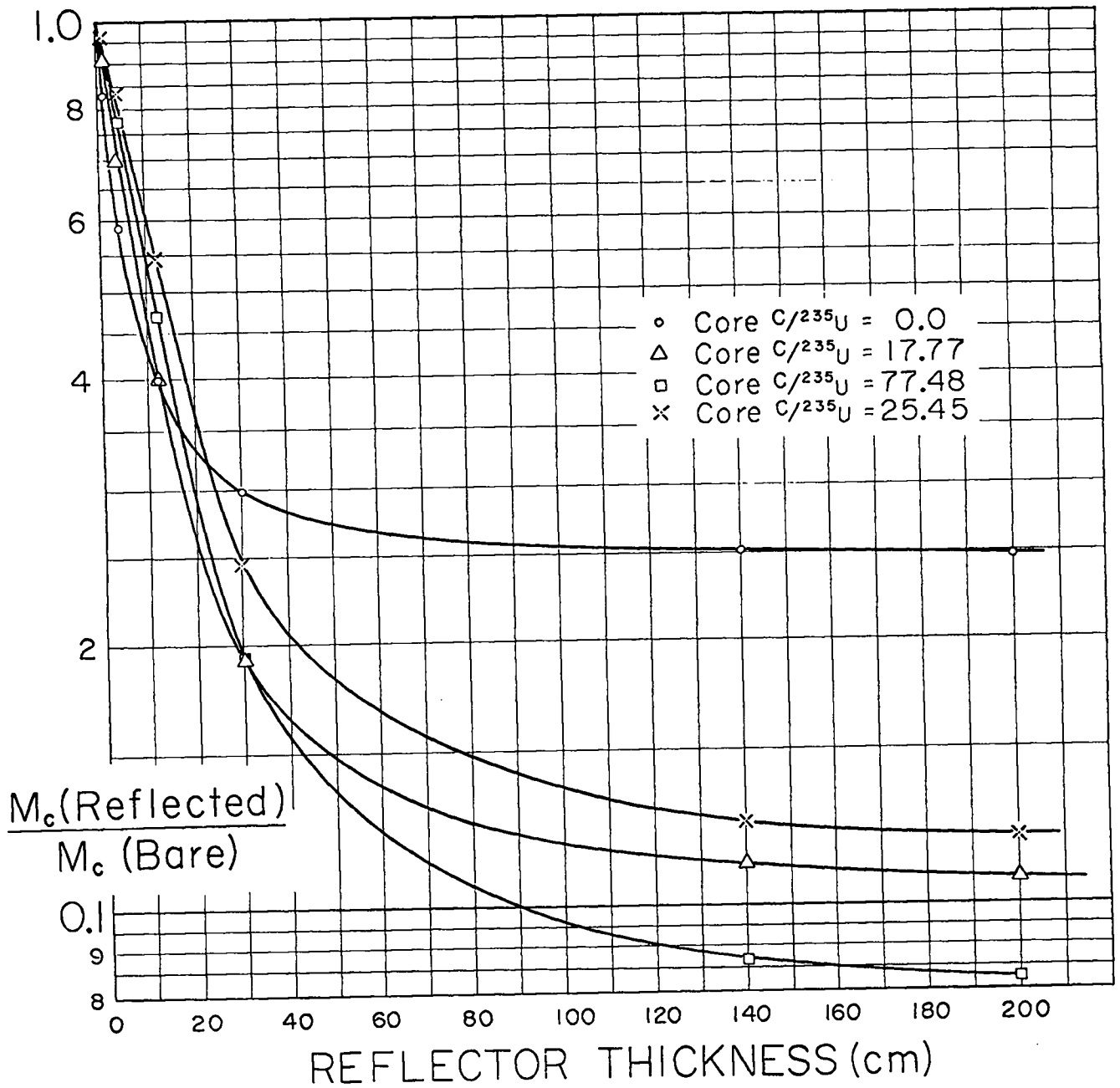


Fig. 20. Calculated ratio of graphite-reflected to bare critical masses for four core mixtures as a function of graphite reflector thickness. For the larger cores, up to 2 meters thickness is required for reflector saturation.

TABLE XX. CRITICAL RADII OF THREE U(93.5) METAL-WATER CORES FOR VARIOUS REFLECTORS

$H/^{235}\text{U}$	$\text{U}^{235}$ Density ( $\text{g}/\text{cm}^3$ )	Reflector Thickness (cm)	Lucite Radius (cm)	Polyethylene Radius (cm)	Water Radius (cm)	Graphite Radius (cm)	Liquid- Hydrogen Radius (cm)
0.0	1.76 +1	0.0	8.652	8.652	8.652	8.652	8.652
0.0	1.76 +1	1.27			8.120	(8.020)	
0.0	1.76 +1	2.54	7.542	7.452	7.655	(7.440)	8.335
0.0	1.76 +1	5.08			7.052	(7.075)	
0.0	1.76 +1	7.62	6.520	6.565	(6.795)	(6.750)	7.929
0.0	1.76 +1	10.16			6.689	(6.510)	
0.0	1.76 +1	15.24	6.351	6.506	(6.640)	(6.195)	
0.0	1.76 +1	25.00	6.346	6.505	6.636	(5.860)	
3.00 +1	8.28 -1	0.0	14.792	14.792	14.792	14.792	14.792
3.00 +1	8.28 -1	1.27			13.765		
3.00 +1	8.28 -1	2.54	12.730	12.478	12.890		14.053
3.00 +1	8.28 -1	5.08			11.720		
3.00 +1	8.28 -1	7.62	10.800	10.878	(11.282)		13.138
3.00 +1	8.28 -1	10.16			11.078		
3.00 +1	8.28 -1	15.24	10.502	10.776	(11.000)		
3.00 +1	8.28 -1	25.40	10.496	10.778	10.994		
3.00 +2	8.65 -2	0.0	16.978	16.978	16.978	16.978	16.978
3.00 +2	8.65 -2	1.27			15.880		
3.00 +2	8.65 -2	2.54	14.889	14.659	15.020		16.116
3.00 +2	8.65 -2	5.09			13.990		
3.00 +2	8.65 -2	7.62	13.217	13.347	(13.620)		15.214
3.00 +2	8.65 -2	10.16			13.500		
3.00 +2	8.65 -2	15.24	12.988	13.269	(13.450)		
3.00 +2	8.65 -2	25.40	12.982	13.264	13.431		

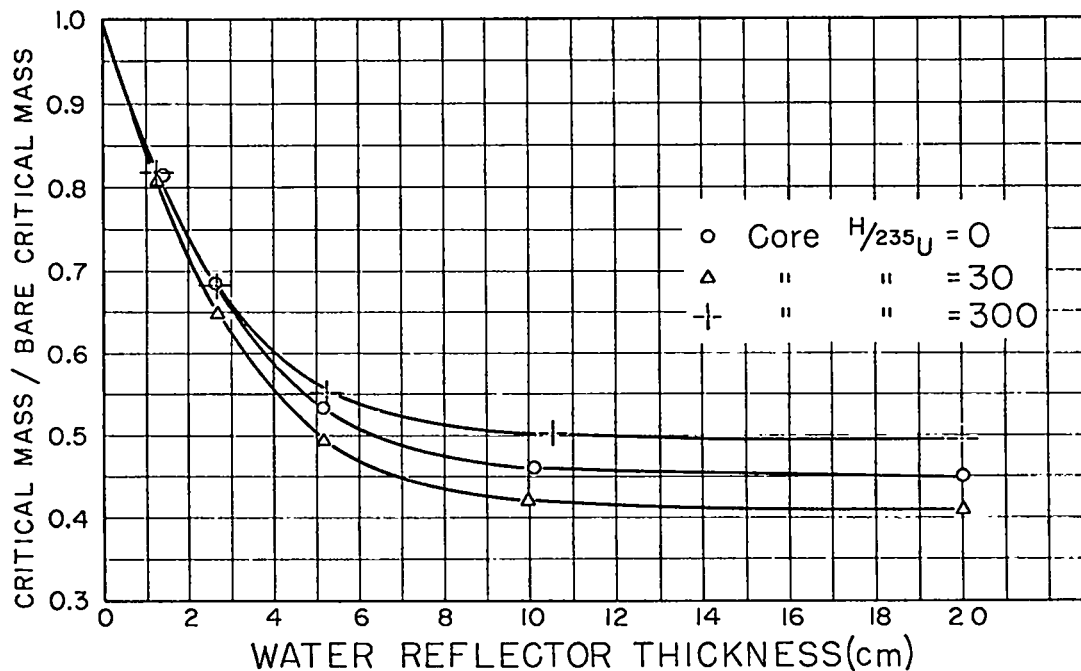


Fig. 21. Calculated ratio of bare to water-reflected critical mass vs water reflector thickness for three U(93.5)-water cores. The hydrocarbon reflectors saturate at about 10 to 12 cm.

TABLE XXI.  $U(1.42)F_4$ -PARAFFIN ASSEMBLY - REFLECTOR SAVING MEASUREMENTS

Material	Thickness (cm)	Reflector Saving		Material	Thickness (cm)	Reflector Saving	
		Bare (cm)	Cd Shielded (cm)			Bare (cm)	Cd Shielded (cm)
Polyethylene	1.3	1.4	1.3	Water	1.5	1.	0.5
	2.7	2.6	1.6		2.9	2.	
	5.4	3.7	1.7		3.8		0.9
	10.8	4.1	1.7		4.5	2.8	
	16.2		1.8		6.4		1.0
	21.5	4.1	1.8		6.7	3.4	
Concrete	2.5	1.4	1.5	Aluminum	9.7	3.5	
	5.1	2.5	2.2		2.5	0.8	0.7
	7.6	3.3	2.5		7.6	1.9	1.6
	10.2		2.7		15.2	2.9	2.4
	12.7	4.4	3.0		22.9	3.4	2.7
	17.8		3.1		30.5	3.7	2.9
Lucite	20.3	5.0	3.2	Mild Steel	40.6	3.7	
	1.3	1.6	1.0		1.3	1.2	1.0
	2.6	2.8	1.4		2.5	1.7	1.6
	3.9	3.5	1.6		3.8	2.5	
	5.2	4.2	1.7		5.1	3.1	2.4
	7.8	4.8	1.7		6.4	3.2	
	9.1	4.9			7.6	3.7	2.9
	10.4	5.1	1.8		8.9	3.9	
	13.0	5.2			10.2	4.1	3.2
	15.6	5.3	1.8		11.4	4.3	
	20.8	5.3			12.7	4.4	3.4
26.0	5.3	1.8	17.8	4.8			
Graphite	2.5	1.6		21.6	5.1		
	6.1	3.5		25.4	5.2	3.8	
	20.3	9.4					
	40.6	13.0					
	61.0	13.9					

Another useful quantity is the change in reflector effectiveness as a gap is opened between core and reflector. Except in the slab geometry, a reflector invariably becomes less effective with distance, the amount depending on the core size and composition and the reflector material and thickness. The possible variations are nearly limitless, but to illustrate the effect, three water-reflected,  $U(93.5)$  metal-water spheres ( $H/^{235}U = 0.0, 30.0, \text{ and } 300.0$ ) are examined. In Fig. 23 the ratio of the reflected critical mass to the bare critical mass is plotted against the gap thickness between the core and reflector. Again, the effectiveness of the water in any position depends on its thickness; in Fig. 23 this is about 20 cm, essentially infinite.

In Section III the concept of a "density exponent" was defined, and some data for water-moderated and water-reflected cores were presented in Figs. 2, 3, and 4. The data pertinent to Fig. 4 (reflector density exponents) are presented in Table XXII; metal-water cores whose  $H/^{235}U$  ratios are 0.0, 30.0, and 300 are reflected by thick water of densities 1.0, 0.8, and 0.4. As shown in Fig. 4, reflector density exponents may be derived, but they are not constants and must tend to zero as the reflector density approaches zero as a limit. The exponent calculated from the data of Table XXII will be appropriate to a mid-point density, but a more satisfactory scheme is to plot the data and derive the exponent from the curve.

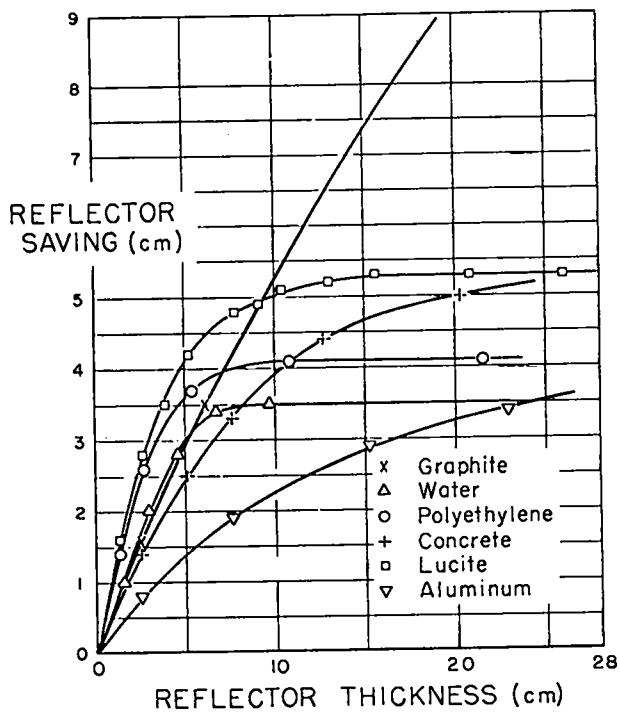


Fig. 22. Experimental reflector saving for several thicknesses of different materials on one face of a large U(1.42)F<sub>4</sub>- paraffin core.

Core density exponents for U(93.5) metal-graphite cores reflected by sundry thicknesses (1, 4, 12, 30, and 100 cm) of graphite ( $\rho = 1.90 \text{ g/cm}^3$ ) may be obtained from the calculated data of Table XXIII. The core, for each reflector thickness, is imagined to be reduced in density to  $\rho = 0.8 \rho_0$  and to  $\rho = 0.4 \rho_0$ . The reflector thickness has been held constant for each triplet of core densities; if reflector volume were invariant, the results would be slightly different and possibly more difficult to interpret. These data are illustrated in Fig. 24 as the ratio of the critical mass at density  $\rho$  to the critical mass at  $\rho_0$  [ $m(\rho)/m(\rho_0)$ ] plotted as a function of the core density ratio ( $\rho/\rho_0$ ). As would be expected, for the very thin reflectors, the core exponent is nearly 2.0; however, for thicknesses of 10 cm or more, the exponent decreases rapidly, and for thicknesses greater than ~30 cm, it cannot even be considered a constant. Extreme changes in the density of a core reflected with graphite

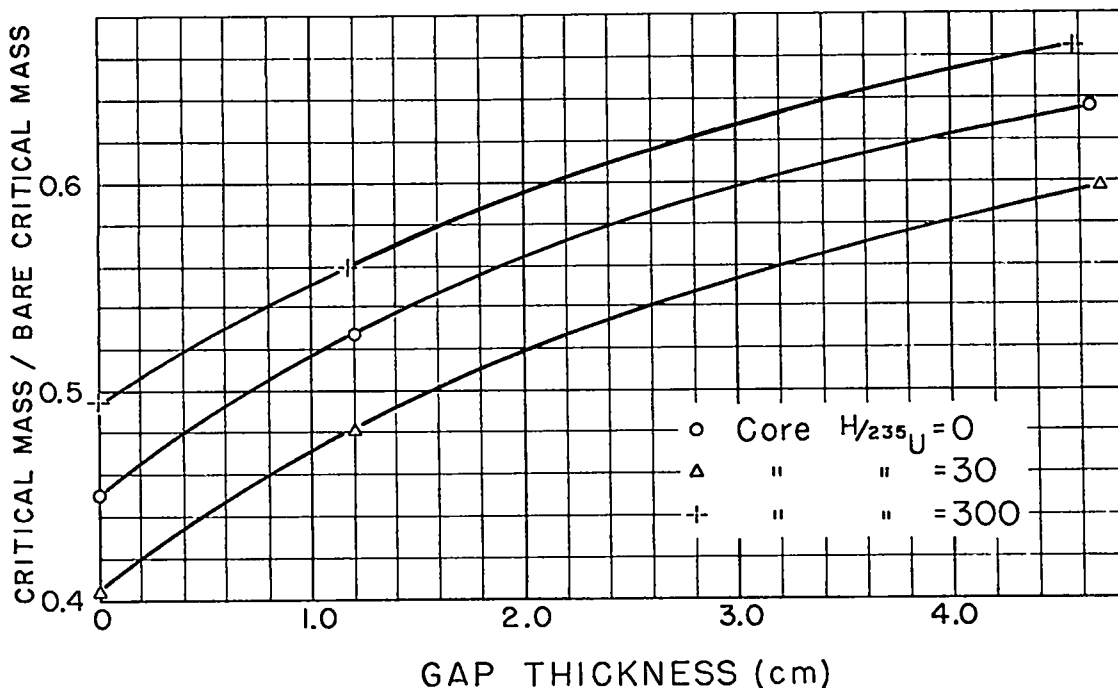


Fig. 23. Computed influence of a gap between the core and water reflector for three U(93.5) metal-water spherical assemblies.

TABLE XXII. CRITICAL RADII OF THREE U(93.5) METAL-WATER CORES;  
WATER REFLECTOR OF VARIABLE DENSITY

$H/^{235}\text{U}$	$^{235}\text{U}$ Density ( $\text{g}/\text{cm}^3$ )	Water Thickness (cm)	Water Density ( $\text{g}/\text{cm}^3$ )	Critical Radius (cm)	Critical Mass, $M(\rho)$ (kg)	$\frac{M(\rho)}{M(\rho_0)}$
0.0	1.76 +1	20.0	1.00	6.636	21.545	1.000
0.0	1.76 +1	20.2	0.80	6.901	24.240	1.125
0.0	1.76 +1	26.5	0.40	7.633	32.790	1.522
3.0 +1	8.28 -1	20.0	1.00	10.994	4.611	1.000
3.0 +1	8.28 -1	21.5	0.80	11.408	5.152	1.117
3.0 +1	8.28 -1	28.7	0.40	12.540	6.843	1.484
3.0 +2	8.65 -2	20.0	1.00	13.431	0.878	1.000
3.0 +2	8.65 -2	21.4	0.80	13.753	0.943	1.074
3.0 +2	8.65 -2	28.1	0.40	14.697	1.150	1.310

TABLE XXIII. U(93.5) METAL-GRAPHITE CORES AT THREE DENSITIES;  
GRAPHITE REFLECTORS OF DIFFERENT THICKNESSES

$C/^{235}\text{U}$	$^{235}\text{U}$ Density ( $\text{g}/\text{cm}^3$ )	Reflector Thickness (cm)	$\rho/\rho_0$ (Core)	Critical Radius (cm)	Critical Mass (kg)	$\frac{M(\rho)}{M(\rho_0)}$
1.777 +1	1.87 +0	1.0	1.00	28.268	177.0	1.00
1.777 +1	1.50 +0	1.0	0.80	35.320	276.3	1.56
1.777 +1	7.48 -1	1.0	0.40	70.556	1101.1	6.22
1.777 +1	1.87 +0	4.0	1.00	25.879	135.8	1.00
1.777 +1	1.50 +0	4.0	0.80	32.153	208.4	1.54
1.777 +1	7.48 -1	4.0	0.40	63.395	798.7	5.88
1.777 +1	1.87 +0	12.0	1.00	21.460	77.5	1.00
1.777 +1	1.50 +0	12.0	0.80	26.001	110.2	1.42
1.777 +1	0.75 -1	12.0	0.40	47.551	337.1	4.35
1.777 +1	1.87 +0	30.0	1.00	16.831	37.4	1.00
1.777 +1	1.50 +0	30.0	0.80	19.442	46.1	1.23
1.777 +1	7.48 -1	30.0	0.40	29.781	82.8	2.21
1.777 +1	1.87 +0	100.0	1.00	14.049	21.7	1.00
1.777 +1	1.50 +0	100.0	0.80	15.649	24.0	1.11
1.777 +1	7.48 -1	100.0	0.40	20.961	28.9	1.33
7.748 +1	4.67 -1	30.0	1.00	25.789	33.59	1.00
7.748 +1	3.74 -1	30.0	0.80	29.919	41.96	1.25
7.748 +1	1.87 -1	30.0	0.40	46.715	79.85	2.38
2.545 +3	1.46 -2	4.0	1.00	56.137	10.83	1.00
2.545 +3	1.17 -2	4.0	0.80	70.024	16.81	1.55
2.545 +3	5.84 -3	4.0	0.40	139.544	66.52	6.14

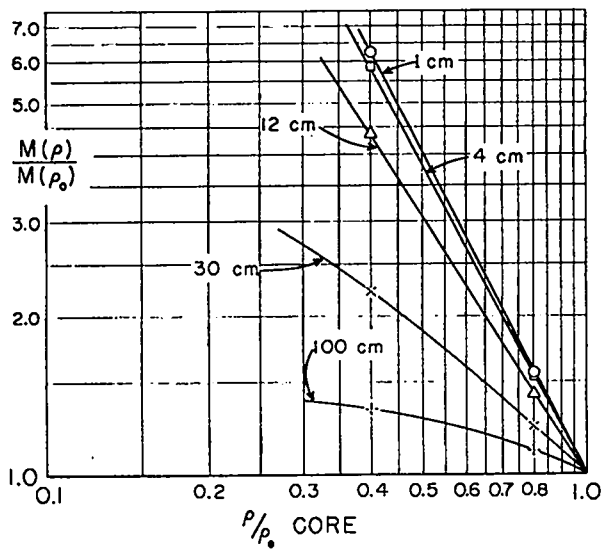


Fig. 24. Computed critical masses for U(93.5)-graphite cores ( $C/^{235}\text{U} = 17.77$ ) as a function of core density for five thicknesses of graphite reflector. Core density exponents may be derived from this figure, but note that for thick reflectors the exponent will not be a constant.

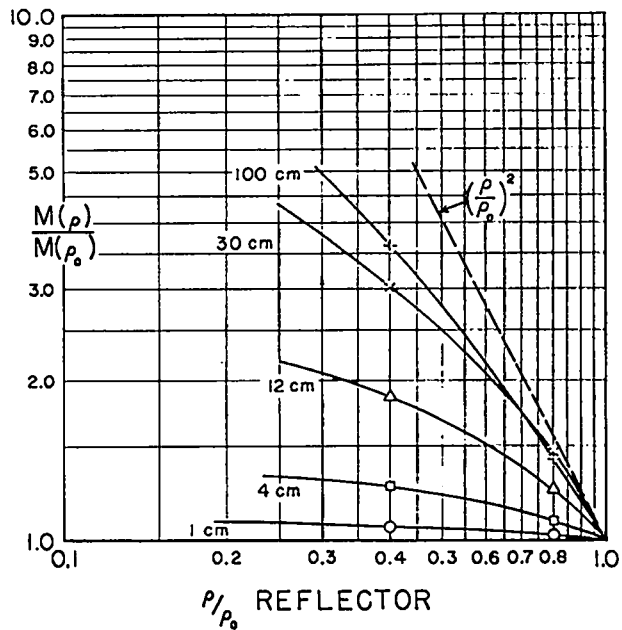


Fig. 25. Computed critical masses for U(93.5)-graphite cores ( $C/^{235}\text{U} = 17.77$ ) as a function of graphite reflector density.

TABLE XXIV. U(93.5) METAL-GRAPHITE CORES;  
GRAPHITE REFLECTOR OF SEVERAL THICKNESSES AND THREE DIFFERENT DENSITIES

$C/^{235}\text{U}$	$^{235}\text{U}$ Density ( $\text{g}/\text{cm}^3$ )	Reflector Thickness (cm)	$\frac{\rho}{\rho_0}$ Reflector	Reflector Density ( $\text{g}/\text{cm}^3$ )	Critical Radius (cm)	Critical Mass (kg)	$\frac{M(\rho)}{M(\rho_0)}$
1.777 +1	1.87 +0	1.0	1.00	1.90	28.268	177.0	1.000
1.777 +1	1.87 +0	1.0	0.80	1.52	28.463	180.7	1.021
1.777 +1	1.87 +0	1.0	0.40	0.76	28.823	187.7	1.060
1.777 +1	1.87 +0	4.0	1.00	1.90	25.879	135.8	1.000
1.777 +1	1.87 +0	4.0	0.80	1.52	26.596	147.4	1.085
1.777 +1	1.87 +0	4.0	0.40	0.76	27.965	171.4	1.262
1.777 +1	1.87 +0	12.0	1.00	1.90	21.460	77.5	1.000
1.777 +1	1.87 +0	12.0	0.80	1.52	23.084	96.4	1.244
1.777 +1	1.87 +0	12.0	0.40	0.76	26.359	143.5	1.852
1.777 +1	1.87 +0	30.0	1.00	1.90	16.831	37.4	1.000
1.777 +1	1.87 +0	30.0	0.80	1.52	19.077	54.4	1.455
1.777 +1	1.87 +0	30.0	0.40	0.76	24.317	112.7	3.013
1.777 +1	1.87 +0	100.0	1.00	1.90	14.049	21.7	1.000
1.777 +1	1.87 +0	100.0	0.80	1.52	15.817	31.0	1.429
1.777 +1	1.87 +0	100.0	0.40	0.76	21.526	78.2	3.602
7.748 +1	4.67 -1	4.0	1.00	1.90	41.122	136.2	1.000
7.748 +1	4.67 -1	4.0	0.80	1.52	41.914	144.2	1.059
7.748 +1	4.67 -1	4.0	0.40	0.76	43.438	160.5	1.178
2.545 +3	1.46 -2	12.0	1.00	1.90	48.795	7.1	1.000
2.545 +3	1.46 -2	12.0	0.80	1.52	51.358	8.3	1.169
2.545 +3	1.46 -2	12.0	0.40	0.76	56.120	10.8	1.521



(also  $D_2O$  and beryllium) will be considered in Section VIIB.

Effects of variation in the reflector density for these same U(93.5) metal-graphite core graphite-reflector combinations are presented in Table XXIV and illustrated in Fig. 25. Again, the display is in the form of a ratio of critical masses plotted against the ratio of densities in the reflector. The low density limit must be the bare critical mass, thus giving a fourth point to each curve in Fig. 25. As in the case for the core variations, the reflector thickness has been held constant for each triplet of critical data. Note that if reflector density exponents are to be extracted for these systems, the reflector thicknesses of each triplet should be adjusted to have a constant neutron mean free path (constant reflector  $g/cm^2$ ).

#### B. Thick Moderating Reflectors (Metastable Systems)

Large changes of core density within a very thick moderating and noncapturing reflector can sometimes introduce an instability previously noticed, but not, to my knowledge, discussed. The effect is illustrated in Fig. 26 in which the critical mass of U(93.5) metal as reflected by thick graphite or beryllium is plotted against

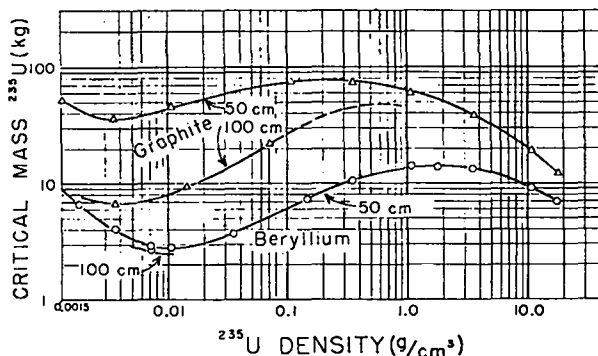


Fig. 26. Computed critical masses of U(93.5) metal reflected by thick graphite or beryllium for a wide range of  $^{235}U$  densities. Note that these systems can be critically unstable in the region in which critical mass decreases with decreasing density.

the  $^{235}U$  metal density in the core -- the core is not diluted, only reduced in density. In a similar manner U(93.5) metal and U(93.5) metal-graphite cores reflected by thick heavy water ( $D_2O$ ) are shown in Fig. 27. The region of core density in which the critical mass is decreasing as the core density decreases may be described as critically unstable -- a critical system here gains reactivity as fission fragments deposit heat energy and cause the core to expand. This interesting autocatalytic process can continue until the reflector is too thin to return sufficient neutrons to maintain the critical state or until the core density is sufficiently low that the critical mass is again increasing as core density is decreasing, but this time without limit.

These data (all calculated) are extreme extensions of the core density variations already discussed. In terms of a core density exponent (defined in Section III), this "constant" passes through zero at that point where the critical mass is independent of the core density; at lower densities the exponent is negative -- the critical mass decreases with decreasing density, but the lower limit to the core

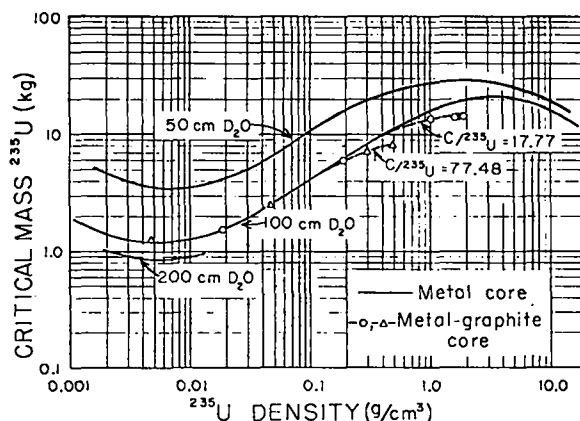


Fig. 27. Computed critical masses of U(93.5) metal and U(93.5) metal-graphite cores surrounded by three thicknesses of  $D_2O$ . At sufficiently low densities, the core graphite has little influence on critical mass. The instability mentioned in the caption for Fig. 26 also pertains to the systems of this figure.

density exponent must be  $-1.0$ , as at this value the critical volume is not dependent upon the core density. A lower number would imply a decreasing volume with decreasing density, a physically impossible situation. As the core density is further reduced, the critical mass passes through a minimum (the exponent again equals zero) at densities between  $0.005$  and  $0.01 \text{ g/cm}^3$ , densities characteristic of a gas. At still lower densities the exponent takes on positive values again and is thought to increase monotonically and approach  $2.0$  as a limit.

Reactors constructed such that the core density is near the minimum in the critical mass are known as Bell cavities or cavity reactors.<sup>(70)</sup> The one extant critical assembly of this type simulates a U(93.5) gas by use of very thin metal foils wrapped around a hollow cylindrical cavity about one meter high and one meter in diameter. The average core density is  $\sim 7.0 \times 10^{-3} \text{ g/cm}^3$ , leading to a critical mass of  $5.8 \text{ kg } ^{235}\text{U}$ . The reflector is  $\text{D}_2\text{O}$ ,  $50\text{-cm}$  thick, substantially less than the infinite thickness. These Bell cavities have been studied intensively by Safonov<sup>(71,72)</sup> and Mills.<sup>(73)</sup>

## VIII. NEUTRON POISONS

As was mentioned earlier the effects of neutron poisons will be treated only cursorily. Most isotopes will act as a mild poison under some circumstances -- primarily depending upon the neutron spectrum or the position of the material in the system. An interesting example of the spectral effect is the poisoning by hydrogen in very thermal neutron systems. This can be seen clearly in Fig. 19 in which the asymptote for water-moderated U(93.5) is at a much higher density than the asymptotes for the isotopes with substantially lower thermal capture cross section -- even though hydrogen is by far the best moderator. An example of the influence of position can

be seen in Fig. 6. Stainless steel is an effective reflector for bare cores but is definitely a poison when placed between a water reflector and the core. Two isotopes of special importance to plutonium solutions are  $^{240}\text{Pu}$  and nitrogen, each of which is a mild poison. The influence of  $^{240}\text{Pu}$  is illustrated in Fig. 17, and that for nitrogen in the form of  $\text{HNO}_3$  can be seen in Fig. 18.

The influence of the "strong" poisons,  $^6\text{Li}$  and  $^{10}\text{B}$ , uniformly mixed in U(93.5) metal (fast neutron) systems<sup>(30)</sup> is to be found in Table IV. These two isotopes are the only ones which can create a dilution exponent for the metal core greater than the bare core density exponent,  $2.0$ . For thermal reactors, these, as well as cadmium,  $^3\text{He}$ , samarium, europium, and gadolinium, are regarded as strong poisons.

A meaningful scheme for establishing a measure of the effectiveness of a poison is to start with a given system, say a  $\text{UO}_2\text{F}_2$  water solution, and ask what ratio of  $^{235}\text{U}$ /poison atoms will just hold the system critical at constant volume. As a soluble poison is added, more U(93.5) as a salt must be inserted (and average solution removed) to just maintain a critical system. Critical data,<sup>(13)</sup> experimental and calculated, for two slightly overmoderated systems are given in Table XXV in which boric acid is balanced by  $^{235}\text{UO}_2(\text{NO}_3)_2$  or  $^{233}\text{UO}_2(\text{NO}_3)_2$ . Similar data may be deduced for plutonium solutions from Fig. 18. In this latter case the poison is nitrogen in the form of  $\text{HNO}_3$ .

An extension of this last concept is to systems of unlimited size, and one asks for the boron concentration that will reduce  $k_\infty$  to  $1.0$ . Experimental data<sup>(74)</sup> are available for U(3.04) $\text{O}_3$  polyethylene mixtures, and the  $\text{B}/^{235}\text{U}$  atom ratio required to hold the  $k_\infty$  of this material to  $1.0$  is shown as a function of the  $\text{H}/^{235}\text{U}$  atom ratio in Fig. 28. The most reactive mixture (at  $\text{H}/^{235}\text{U} \sim 270$ ) requires  $0.365$  boron at-

TABLE XXV. EXPERIMENTAL AND COMPUTED PARAMETERS FOR SPHERES OF  $UO_2(NO_3)_2$   
SOLUTION PLUS BORON

$^{235}U$					
$H/^{235}U$	$B/^{235}U$	$^{235}U$ Density ( $g/cm^3$ )	Sphere Radius (cm)		$\frac{R_{DTK}}{R_{Exp}}$
			Observed	Computed	
1.38 +3	0.0	1.88 -2	34.60	33.75	0.975
1.18 +3	9.25 -2	2.19 -2	34.60	33.78	0.976
1.03 +3	1.63 -1	2.50 -2	34.60	--	--
9.72 +2	1.88 -1	2.65 -2	34.60	33.92	0.980

$^{233}U$					
$H/^{233}U$	$B/^{233}U$	$^{233}U$ Density ( $g/cm^3$ )	Sphere Radius (cm)		$\frac{R_{DTK}}{R_{Exp}}$
			Observed	Computed	
1.53 +3	0.0	1.68 -2	34.60	33.94	0.981
1.47 +3	2.95 -2	1.75 -2	34.60	--	--
1.42 +3	5.53 -2	1.81 -2	34.60	33.96	0.982
1.37 +3	7.90 -2	1.87 -2	34.60	--	--
1.32 +3	1.02 -1	1.94 -2	34.60	33.99	0.982

oms for each  $^{235}U$  atom to reduce  $k_{\infty}$  to unity, while the unpoisoned system is just critical at  $H/^{235}U \sim 1.0$  and  $\sim 1410$ . Cal-

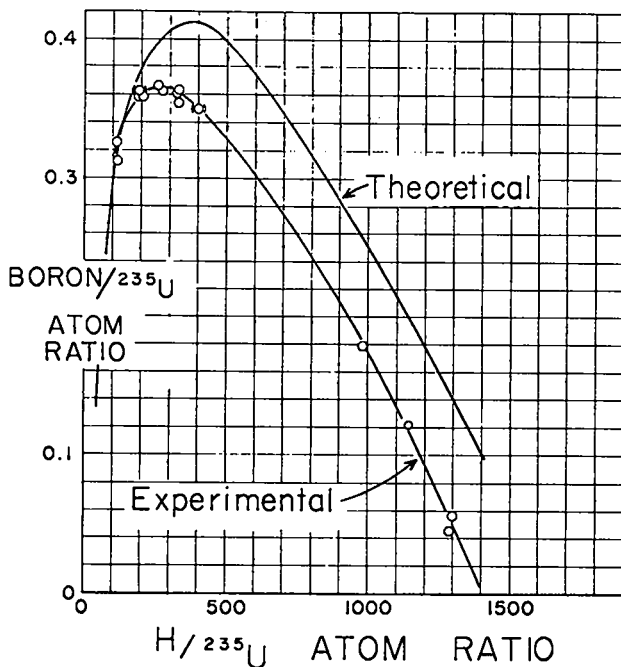


Fig. 28. Experimental and computed boron concentrations to maintain  $k_{\infty} = 1.0$  in hydrogen-moderated U(3).

culational results<sup>(31)</sup> are included in Fig. 28. For moderation ratios greater than  $\sim 150$ , the calculation is conservative in the criticality safety sense.

A study<sup>(13)</sup> has been completed which defines the boron-to-fissile atom ratio for  $k_{\infty} = 1.0$  for water-moderated systems of U(93.2),  $^{239}Pu$ , and  $^{233}U$ . These calculated results are illustrated on Fig. 29. Because small changes in the scattering prop-

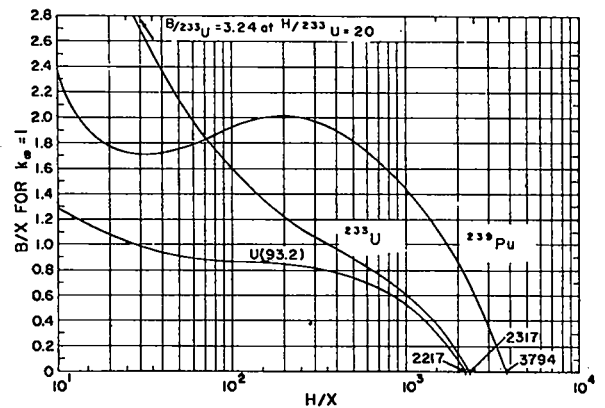


Fig. 29. Computed boron concentrations to maintain  $k_{\infty} = 1.0$  for water-moderated systems of U(93.5),  $^{239}Pu$ , and  $^{233}U$ . At  $H/^{233}U = 20$ , the  $B/^{233}U$  atom ratio is 3.24.

erties of the moderator can cause large changes in the B/X ratio, these data, especially at low moderations should be used with caution.

#### IX. SUMMARY AND CONCLUSIONS

Broad generalizations as to the overall accuracy of the calculation and of the completeness of the set of experimental data will be avoided; however, some comments on specific points, general trends, and areas of usefulness may be noted.

A satisfactory result is that the theory (DSN code plus 16-group cross sections) is successful for the calculation of highly enriched  $^{235}\text{U}$  thermal systems, even though the cross sections were originally chosen for application to fast and epithermal cores. The transition from fast to slow neutron systems is also accurately described, as comparisons with the meager experimental data in this intermediate area seem to indicate.

A tendency for a progressive overestimate of critical radii with decreasing enrichment is seen; this difficulty is thought to be buried in the  $^{238}\text{U}$  cross sections. A similar trend (but less well-established) toward increasing error with decreasing H/ $^{235}\text{U}$  ratio for the systems enriched to 5%  $^{235}\text{U}$  or less is also noticed. Additional investigation, both experimental and theoretical, of these problems seems justified. It is likely that Pu- $^{238}\text{U}$  systems will be calculated with similar errors.

Theoretical difficulties seem to be connected with water-reflected  $^{233}\text{U}$  systems, while an obvious (but not unique) need is seen for more experiments with slightly moderated plutonium cores. The influence of  $^{240}\text{Pu}$  is most inadequately known experimentally. Without drawing attention to more specific areas, I note that numerous precise experiments are still needed.

Many of the calculated density exponent and reflector saving data are new. I see no reason to suspect that these are grossly inaccurate, and application with reasonable care seems appropriate.

I fully expect that some basic, accurate, and important data have been omitted; I assure the originators that the slight is not intentional and enlightenment is welcomed. Indeed, if data are uncovered because of this report, one major objective will have been achieved. Some experimental and theoretical results are published herein for the first time, and for this privilege I am most grateful.

#### ACKNOWLEDGMENTS

It is a pleasure to thank H. C. Paxton and A. D. Callihan for their interest, encouragement, and very considerable and patient assistance in the preparation of this review. It would have been quite impossible except for their earlier and extensive work in the field. The very generous and continued assistance and advice of G. E. Hansen is especially noted; I call attention again to the fact that all critical-radius and k calculations published herein have been completed using the Hansen-Roach cross-section set. Group T-1 at LASL has, without complaint, set up and run a great many DSN problems for this review on the 7094 computer. The theoretical specifications and subsequent analysis of many computations and parametric studies are due to P. M. Wallis. And last, but not least, I am most grateful to Mrs. Thelma Thomas for the figures and to Mrs. Jean Frame and Mrs. Antonia Flores for their patient typing and retyping of the manuscript.

REFERENCES

1. R. F. Christy and J. A. Wheeler, Chain Reaction of Pure Fissionable Materials in Solution, University of Chicago, Metallurgical Laboratory report CP-400, January 1, 1943. In this document a letter (December 1942) from J. R. Oppenheimer is quoted in which he and R. Serber also estimated the critical masses of  $^{235}\text{U}$  and  $^{239}\text{Pu}$  in water solution.
2. R. Serber, The Los Alamos Primer, Notes written up by E. U. Condon, Los Alamos Scientific Laboratory report LA-1, April 1943.
3. H. C. Paxton, Los Alamos Critical-Mass Data, Los Alamos Scientific Laboratory report LAMS-3067, April 1964.
4. C. P. Baker et al., Water Boiler, Los Alamos Scientific Laboratory report LA-134, September 1944.
5. L.D.P. King, Critical Assemblies Part II, Los Alamos Scientific Laboratory report LA-1034, Volume V, Chapter 4, December 1947.
6. B. Carlson, C. Lee, and J. Worlton, The DSN and TDC Neutron Transport Codes, Los Alamos Scientific Laboratory report LAMS-2346, October 1959.
7. Bengt G. Carlson, Numerical Solution of Transient and Steady-State Neutron Transport Problems, Los Alamos Scientific Laboratory report LA-2260, May 16, 1959.
8. Bengt G. Carlson, The Numerical Theory of Neutron Transport, Methods in Computational Physics, Volume 1, Academic Press, New York (1963).
9. B. G. Carlson and G. I. Bell, Solution of the Transport Equation by the  $S_n$  Method, Proc. U. N. Intern. Conf. Peaceful Uses At. Energy, 2nd, Geneva, 1958, 16, 535 (1958).
10. Gordon E. Hansen and William H. Roach, Six and Sixteen Group Cross Sections for Fast and Intermediate Critical Assemblies, Los Alamos Scientific Laboratory report LAMS-2543, November 1961.
11. G. Safonov, Survey of Reacting Mixtures Employing  $^{235}\text{U}$ ,  $^{239}\text{Pu}$ , and  $^{233}\text{U}$  for Fuel and  $\text{H}_2\text{O}$ ,  $\text{D}_2\text{O}$ , C, Be, and BeO for Moderator, The Rand Corporation report R-259, 1954.
12. C. B. Mills, Minimum Critical Dimensions for Water Solutions, Nucl. Sci. Eng. 9, 377 (1961).
13. William H. Roach, Parametric Survey of Critical Sizes, Pergamon Press, Progress in Nuclear Energy, Technology, Engineering, and Safety, Vol. 5, page 505, (1963).
14. C. B. Mills and G. I. Bell, Criticality of Low Enrichment Uranium in Hydrogen, Nucl. Sci. Eng. 12, 469 (1962).
15. Gordon E. Hansen, Los Alamos Scientific Laboratory, private communication.
16. Samuel Glasstone and Milton C. Edlund, The Elements of Nuclear Reactor Theory, D. Van Nostrand Company, Inc., New York (1952).
17. G. E. Hansen, D. P. Wood, and B. Peña, Reflector Savings of Moderating Materials on Large Diameter U(93.2) Slabs, Los Alamos Scientific Laboratory report LAMS-2744, June 1962.
18. H. C. Paxton, Critical Dimensions of Systems Containing  $^{235}\text{U}$ ,  $^{239}\text{Pu}$ , and  $^{233}\text{U}$ , USAEC Technical Information Service document TID-7028, 1964.
19. G. E. Hansen, private communication. A special series of two-dimensional problems were completed to study this problem.
20. Bengt G. Carlson and William J. Worlton, Los Alamos Scientific Laboratory, private communication.
21. R. Serber, The Los Alamos Primer, Los Alamos Scientific Laboratory report LA-1, April 1943, page 7. See also reference 23 for a discussion of this subject.
22. C. M. Nicholls, E. R. Woodcock, and A. H. Gillieson, Criticality, Chapter IX of Chemical Processing of Reactor Fuels, edited by John F. Flagg; Academic Press, New York (1961).
23. J. D. Orndoff, H. C. Paxton, and G. E. Hansen, Critical Masses of Oy at Reduced Concentrations and Densities, Los Alamos Scientific Laboratory report LA-1251, May 1951. This reference contains some discussion of the earlier development of this concept. The origin is obscure.
24. Aubrey Thomas and R. C. Lane, UKAEA Atomic Weapons Research Establishment, Aldermaston, private communication.
25. A. D. Callihan et al., Critical Mass Studies, Part V, Oak Ridge National Laboratory report K-643, June 1950.
26. G. A. Linenberger, J. D. Orndoff, and H. C. Paxton, Enriched-Uranium Hydride Critical Assemblies, Nucl. Sci. Eng. 7, 44 (1960).
27. C. R. Richey et al., Critical Experiments with  $\text{PuO}_2$ -Polystyrene Compacts, Hanford Atomic Products Operation report HW-80020, January 1964.
28. William R. Stratton, Critical Dimensions of U(93.5)-Graphite-Water Spheres, Cylinders, and Slabs, Los Alamos Scientific Laboratory report LAMS-2955, May 1962.
29. D. P. Wood, C. C. Byers, and L. C. Osborn, Critical Masses of Cylinders of Plutonium Diluted with Other Metals, Nucl. Sci. Eng. 8, 578 (1960).

30. L. B. Engle, G. E. Hansen, and H. C. Paxton, Reactivity Contributions of Various Materials in Topsy, Godiva and Jezebel, Nucl. Sci. Eng. 8, 543 (1960).
31. Peter M. Wallis, Los Alamos Scientific Laboratory, private communication.
32. George A. Jarvis, Los Alamos Scientific Laboratory, private communication.
33. A. J. Kirschbaum, Studies of Enriched Uranium Graphite Systems, Lawrence Radiation Laboratory report UCRL-4983-T, November 1957.
34. J. E. Schwager, F. A. Kloverstrom, and W. S. Gilbert, Critical Measurements on Intermediate-Energy Graphite-U<sup>235</sup> Systems, Lawrence Radiation Laboratory report UCRL-5006, November 1957.
35. H. L. Reynolds, Critical Mass Measurements on Graphite U<sup>235</sup> Systems, Proc. U. N. Intern. Conf. Peaceful Uses At. Energy, 2nd, Geneva, 1958, 12, 632 (1958).
36. C. K. Beck, A. D. Callihan, J. W. Moffitt, and R. L. Murray, Critical Mass Studies, Part III, Oak Ridge National Laboratory report K-343, April 1949.
37. J. K. Fox, L. W. Gilley, and A. D. Callihan, Critical Mass Studies, Part IX, Aqueous U<sup>235</sup> Solutions, Oak Ridge National Laboratory report ORNL-2367, February 1958.
38. J. K. Fox et al., Critical Parameters of U<sup>235</sup> and U<sup>233</sup> Solutions in Simple Geometry, Oak Ridge National Laboratory report ORNL-2842, September 1959.
39. J. K. Fox et al., Critical Parameters of Uranium Solutions in Simple Geometry, Oak Ridge National Laboratory report ORNL-2609, February 1958.
40. J. K. Fox, L. W. Gilley, and J. H. Marble, Critical Parameters of a Proton-Moderated and Proton-Reflected Slab of U<sup>235</sup>, Nucl. Sci. Eng. 3, 694 (1958). Extrapolation of these experimental data to the infinite slab geometry was performed on an equal buckling basis. The infinite slab thickness is substantially different from that deduced in the journal article.
41. J. K. Fox, Critical Parameters of Solutions of U<sup>235</sup>-Enriched Uranyl Nitrate in Cylindrical Containers, Oak Ridge National Laboratory report ORNL-3193, September 1961.
42. R. Gwin and D. W. Magnuson, Critical Experiments for Reactor Physics Studies, Oak Ridge National Laboratory report ORNL-CF-60-4-12, September 1960.
43. J. G. Walford and J. C. Smith, UKAEA Dounreay Experimental Reactor Establishment, Dounreay, private communication.
44. D. Fieno et al., Criticality Effects of Centrally Located Tubes and Rods of Aluminum, Iron, and Tungsten in a Homogeneous Reactor, National Aeronautics and Space Administration document NASA-TN-D-1322, August 1962.
45. S. Weinstein, R. Bobone, and F. Feiner, Catalogue of SHA Experiments and Calculations, Knolls Atomic Power Laboratory report KAPL-M-SW-3, July 1963.
46. J. C. Hoogterp, Los Alamos Scientific Laboratory, private communication.
47. D. F. Cronin, Oak Ridge National Laboratory, private communication.
48. J. T. Thomas and J. J. Lynn, Homogeneous Critical Assemblies of 3% U<sup>235</sup>-Enriched UF<sub>4</sub> in Paraffin, Oak Ridge National Laboratory report ORNL-3193, September 1961.
49. V. I. Neeley and H. E. Handler, Measurement of Multiplication Constant for Slightly Enriched Homogeneous UO<sub>3</sub>-Water Mixtures and Minimum Enrichment for Criticality, Hanford Atomic Products Operation report HW-70310, August 1961. A letter (December 1961) from E. D. Clayton reports the minimum enrichment for  $k_{\infty} = 1.0$  as  $1.03 \pm 0.01$ .
50. J. T. Mihalczko and J. J. Lynn, Homogeneous Critical Assemblies of 2% U<sup>235</sup>-Enriched UF<sub>4</sub> in Paraffin, Oak Ridge National Laboratory report ORNL-3016, September 1960.
51. J. T. Mihalczko and C. B. Mills, Criticality of Low Enrichment U<sup>235</sup> in Hydrogen, Nucl. Sci. Eng. 11, 95 (1961).
52. J. T. Mihalczko and V. I. Neeley, The Infinite Multiplication Constant of Homogeneous Hydrogen-Moderated 2.0 wt. % U<sup>235</sup>-Enriched Uranium, Nucl. Sci. Eng. 13, 6 (1962).
53. J. K. Fox, L. W. Gilley, and E. R. Rohner, Critical Mass Studies, Part VIII, Aqueous Solutions of U<sup>235</sup>, Oak Ridge National Laboratory report ORNL-2143, September 1959.
54. J. K. Fox et al., Critical Parameters of U<sup>235</sup> and U<sup>233</sup> Solutions in Simple Geometry, Oak Ridge National Laboratory report ORNL-2842, September 1959.
55. J. K. Fox et al., Critical Parameters of Uranium Solutions in Simple Geometry, Oak Ridge National Laboratory report ORNL-2609, February 1958.
56. R. Gwin and D. W. Magnuson, Critical Experiments for Reactor Physics Studies, Oak Ridge National Laboratory report ORNL CF-60-4-12, September 1960.
57. F. E. Kreusi, J. O. Erkman, and D. D. Lanning, Critical Mass Studies of Plutonium Solutions, Hanford Atomic Products Operation report HW-24514 (Del.), May 1952.

58. R. C. Lloyd et al., Critical Experiments with Plutonium Nitrate Solutions, Hanford Atomic Products Operation, Quarterly Report Ending March 1963.
59. J. Bruna et al., Alecto, Critical Experiments with a Plutonium Solution, Centre d'Etudes Nucléaires de Saclay, C.E.A. No. 2274, 1963.
60. J. Bruna et al., Centre d'Etudes Nucléaires de Saclay, private communication, 1963.
61. C. L. Schuske et al., Plutonium Plexiglas Assemblies, Rocky Flats Plant report RFP-178, January 1960.
62. G. H. Bidinger, C. L. Schuske, and D. F. Smith, Plutonium Plexiglas Assemblies Part II, Rocky Flats Plant report RFP-190, April 1960.
63. A. Goodwin, Jr., and C. L. Schuske, Plexiglas and Graphite Moderated Plutonium Assemblies, Reactor Sci. Technol. (J. Nucl. Energy, Parts A/B) 15, 120 (1961).
64. R. H. Masterson, J. D. White, and T. J. Powell, The Limiting Critical Concentrations for Pu<sup>239</sup> and U<sup>235</sup> in Aqueous Solutions, Hanford Atomic Products Operation report HW-77089, March 1963.
65. R. N. Olcott, Homogeneous Heavy Water Moderated Critical Assemblies, Part I, Experimental, Nucl. Sci. Eng. 1, 327 (1956).
66. H. Hurwitz, Jr., and R. Ehrlich, Comparison of Theory and Experiment for Intermediate Assemblies, Proc. Intern. Conf. Peaceful Uses At. Energy, Geneva, 1955, 5, 423 (1955).
67. F. A. Kloverstrom, R.M.R. Deck, and A. J. Reyenga, Critical Measurements on Near-Homogeneous BeO-Moderated, Orally-Fueled Systems, Nucl. Sci. Eng. 8, 221 (1960).
68. J. R. Morton, III, and E. Goldberg, Pulsed Neutron Measurements on Solid, Moderated, Enriched Uranium Subcritical Assemblies, University of California Radiation Laboratory report UCRL-12013, July 1964.
69. C. B. Mills, Los Alamos Scientific Laboratory, private communication.
70. G. I. Bell, Calculations of the Critical Mass of UF<sub>6</sub> as a Gaseous Core with Reflectors of D<sub>2</sub>O, Be and C, Los Alamos Scientific Laboratory report LA-1874, February 1954.
71. G. Safonov, Externally Moderated Reactors, The Rand Corporation report R-316, July 1957.
72. G. Safonov, Externally Moderated Reactors, Proc. U. N. Intern. Conf. Peaceful Uses At. Energy, 2nd, Geneva, 1958, 12, 705 (1958).
73. C. B. Mills, Reflector Moderated Reactors, Nucl. Sci. Eng. 13, 301 (1962).
74. V. I. Neeley, J. A. Berberet, and R. H. Masterson, k<sub>∞</sub> of Three Weight Percent U<sup>235</sup> Enriched UO<sub>3</sub> and UO<sub>2</sub>(NO<sub>3</sub>)<sub>2</sub> Hydrogenous Systems, Hanford Atomic Operations report HW-66882, 1961.

SEP 25 1967

RECEIVED  
LASL LIBRARIES